As of 10 June 2016

This GOES-R Level 2+ space weather Algorithm Theoretical Basis Document (ATBD) is preliminary and subject to change as the GOES-R Program prepares for a launch in late 2016.

The NOAA National Centers for Environmental Information (NCEI) is currently developing a demonstration version of the Satellite Product Analysis and Distribution Enterprise System (SPADES) which will host the L2+ algorithms. The operational SPADES will be instantiated by the National Weather Service in FY2017 to serve the needs of the Space Weather Prediction Center (SWPC).

Updated versions of the L2+ ATBDs will periodically be made available and posted to the SPADES website.

Bill Denig
NCEI

http://www.ngdc.noaa.gov/stp/space-weather/online-publications/stp_sii/spades/

NOAA NESDIS
CENTER for SATELLITE APPLICATIONS and RESEARCH

GOES R SEISS DIFFERENTIAL-TO-INTEGRAL FLUX ALGORITHM THEORETICAL BASIS DOCUMENT
Version 1.0

Hardcopy Uncontrolled

TITLE: SEISS DIFFERENTIAL-TO-INTEGRAL FLUX ALGORITHM THEORETICAL BASIS DOCUMENT VERSION 1.0

AUTHORS:
Juan V. Rodriguez
Leslie Mayer
Terrance G. Onsager
Jennifer Gannon

APPROVAL SIGNATURES:

<Actual Signature Date>
Mary Shouldis Date
Project Development Lead

<Actual Signature Date>
Steven Hill Date
Project Manager

<Actual Signature Date>
Janet Green Date
Instrument Scientist

SEISS DIFFERENTIAL-TO-INTEGRAL FLUX ALGORITHM THEORETICAL BASIS DOCUMENT VERSION HISTORY SUMMARY

Version	**Description**	**Revised Sections**	**Date**
1.0	Created by Juan Rodriguez CIRES/SWPC	New Document	November 6, 2009

TABLE OF CONTENTS

TABLE OF CONTENTS 7
LIST OF FIGURES 9
LIST OF TABLES 11
LIST OF ACRONYMS 12
ABSTRACT 13
1.0 INTRODUCTION 14
1.1 Purpose of This Document 14
1.2 Who Should Use This Document 14
1.3 Inside Each Section 14
1.4 Related Documents 15
1.5 Revision History 15
2.0 OBSERVING SYSTEM OVERVIEW 16
2.1 Product Generated 16
2.2 Instrument Characteristics 16
3.0 ALGORITHM DESCRIPTION 18
3.1 Algorithm Overview 18
3.2 Processing Outline 18
3.3 Algorithm Input 19
3.3.1 Primary Sensor Data 19
3.3.2 Ancillary Data 21
3.4 Theoretical Description 23
3.4.1 Physics of the Problem 23
3.4.2 Mathematical Description 26
3.4.3 Considerations in the Presence of Background Counts 34
3.4.4 Algorithm Output 36
4.0 TEST DATA SETS AND OUTPUTS 38
4.1 Simulated/Proxy Input Data Sets 38
4.1.1 Trapped Proton Fluxes in the Lowest Channels 41
4.2 Construction of Simulated Proton Spectra 41
4.3 Test Results Using Simulated Proton Spectra, including Uncertainty Estimates ... 45
5.0 PRACTICAL CONSIDERATIONS 56
5.1 Numerical Computation Considerations 56
5.2 Programming and Procedural Considerations 56
5.3 Quality Assessment and Diagnostics 56
5.4 Exception Handling 57
5.5 Algorithm Validation 58
6.0 ASSUMPTIONS AND LIMITATIONS 59
6.1 Instrument Characteristics 59

6.2 Instrument Constants to be Re-evaluated after Cal/Val 59
6.3 Input and Output File Contents and Formats 60
6.4 Performance 60
6.5 Pre-Planned Product Improvements 61
7.0 REFERENCES 62

LIST OF FIGURES

Figure 1. Minimum and maximum proton spectra specified in SEISS PORD for MPS-Hi and SGPS. 25

Figure 2. Rapid evolution of the 100-600 MeV spectrum of solar protons at 7-minute intervals during the onset of the SEP event of September 28, 1961, as measured by Explorer 12 [after Bryant et al., 1962, Figure 11]. 25

Figure 3. Description of a subsection of the integral flux spectrum 26

Figure 4. Comparison of GOES-R resampled proxy data with original GOES 8 and 10 data, for solar proton spectrum measured at 12 UT on September 24 and 26, 2001..... 39

Figure 5. Comparison of GOES 8 (westward) and GOES 10 (eastward) observations of solar proton differential fluxes and least-squares fits to a kappa function without (left) and with (right) a power law component at the lowest energies with $\gamma = 5.5$..... 44

Figure 6. Comparison of integral flux and differential flux retrievals to “truth” for the GOES 8 westward observations of solar protons during the September 24, 2001 SEP event. 46

Figure 7. Comparison of integral flux and differential flux retrievals to “truth” for the GOES 10 eastward observations of solar protons during the September 24, 2001 SEP event. 47

Figure 8. Comparison of integral flux and differential flux retrievals to “truth” for the GOES 8 westward observations of solar protons during the November 22, 2001 SEP event. 48

Figure 9. Comparison of integral flux and differential flux retrievals to “truth” for the GOES 10 eastward observations of solar protons during the November 22, 2001 SEP event. 49

Figure 10. Comparison of integral flux and differential flux retrievals to “truth” for the GOES 11 westward observations of solar protons during the July 25, 2004 SEP event. 50

Figure 11. Comparison of integral flux and differential flux retrievals to “truth” for the GOES 10 eastward observations of solar protons during the July 25, 2004 SEP event. 51

Figure 12. Comparison of integral flux and differential flux retrievals to "truth" for the GOES distribution to the GOES 11 data. 52

Figure 13. Comparison of integral flux and differential flux retrievals to "truth" for the GOES 10 eastward observations of solar protons during the December 6, 2006 SEP event. 53

Figure 14. Percent RMS error for each of the integral flux retrievals shown in Figure 6 through Figure 13..... 54

Figure 15. Percent RMS error for each of the differential flux retrievals shown in Figure 6 through Figure 13. 55

LIST OF TABLES

Table 1. L1b (5-minute-averaged) inputs to SEISS Differential-to-Integral Flux algorithm for a single SGPS FOV (east or west). 20

Table 2. Potential SEISS SGPS L1b metadata to be considered for pass through to the L2 integral flux data records in future versions. 21

Table 3. Ancillary data related to SGPS performance characteristics required by the SEISS L2 Differential-to-Integral Flux algorithm. 22

Table 4. Additional ancillary data related to SGPS performance characteristics that are needed for L2 cal/val. 22

Table 5. Various GOES I-P constants used in determining and applying the background correction by the Zwickl [1989] algorithm. 35

Table 6. The quantities from Table 5, interpolated to the SGPS channels.. 35

Table 7. Level 2 Outputs of SEISS Differential-to-Integral Flux Algorithm. 36

Table 8. Test Cases (SEP onsets and active region location from “Solar Proton Events Affecting the Earth Environment, January 1976 – July 2007,” at http://www.swpc.noaa.gov/ftpdir/indices/SPE.txt)..... 38

Table 9. GOES-R SGPS proton channel energies used as initial guesses in L2 Algorithm. 40

Table 10. GOES I-P EPS/EPEAD proton channel energies as documented by Zwickl [1989] and used in the operational processing code. 40

LIST OF ACRONYMS

AIT	AWG Integration Team
ATBD	Algorithm Theoretical Basis Document
AWG	Algorithm Working Group
CIRES	Cooperative Institute for Research in Environmental Sciences
eV	electron volt
FOV	field-of-view
keV	kilo-electron-volt
L1b	Level 1b
L2	Level 2
MeV	mega-electron-volt
pfu	particle flux unit
PORD	Performance and Operational Requirements Document
SEISS	Space Environment In-Situ Suite
SEP	solar energetic particle (event)
SGPS	Solar and Galactic Proton Sensor
STAR	Center for Satellite Applications and Research
SWPC	Space Weather Prediction Center

ABSTRACT

This document provides a description of the SEISS Level 2 Differential-to-Integral Flux algorithm developed to calculate proton integral flux values using the 5-minute differential proton flux averages determined by algorithm SEISS.17. These averages are constructed from SEISS SGPS Level 1b data. The complete theoretical basis is described, including the fundamental physical assumption of a piecewise power law spectrum. Exception handling is described, including the treatment of fluxes near background levels and limits on the spectral indices. Performance comparisons with the GOES I-P legacy algorithm using theoretical spectra derived from measurements, show that the combination of the new instrument and new algorithm should improve performance substantially over the legacy system. Important assumptions and limitations, particularly concerning input data and metadata, are summarized in the final section.

1.0 INTRODUCTION

1.1 Purpose of This Document

The purpose of this document is to describe the development and design of the SEISS algorithm produced to calculate proton integral flux values from differential flux averages, including details needed for implementation of the algorithm and examples of use and validation. It provides the operational requirements for this product and defines how these requirements are met with this algorithm. The algorithm inputs, processing and outputs are described in enough detail to design, develop, test and implement the necessary processing software and storage mechanisms.

1.2 Who Should Use This Document

The members of the Space Weather Forecast Office and the Research and Customer Requirements Section of the SWPC should use this ATBD to verify that their operational requirements are being met by the proposed algorithm. They should also use it to understand the strengths and weaknesses of the algorithm as well as its accuracy and applicability. The STAR AIT group should use this document to integrate the algorithm into their collaborative framework environment. It should also be used by the ground segment contractor to design, develop, test, validate and implement the algorithm into the final operational processing system.

1.3 Inside Each Section

Section 2.0 OBSERVING SYSTEM OVERVIEW:
Describes the SEISS SGPS instrument and the measurements that serve as input to the algorithm.

Section 3.0 ALGORITHM DESCRIPTION:
Describes the development, theory and mathematics of the algorithm. Describes the logical flow of the algorithm, including input and output flow.

Section 4.0 TEST DATA SETS AND OUTPUTS:
Describes the test data sets used to characterize the performance of the algorithm and the data product quality. Describes the results from the algorithm processing on simulated input data.

Section 5.0 PRACTICAL CONSIDERATIONS:
Discusses issues involving numerical computation, programming and procedures, quality assessment and diagnostics and exception handling.

Section 6.0 ASSUMPTIONS AND LIMITATIONS:
Describes assumptions regarding input data contents and formats; instrument performance and characterization data; and potential future changes and improvements.

Section 7.0 REFERENCES:
Provides all references mentioned in the ATBD.

1.4 Related Documents

GOES-R SEISS Differential-to-Integral Flux Algorithm Implementation and User's Guide, Version 1.0, September xx, 2009.

GOES-R SEISS Differential-to-Integral Flux Algorithm Test Plan and Results, Version 1.0, September xx, 2009.

GOES-R Series Mission Requirements Document (MRD), P417-R-MRD-0070, Version 3.1, December 5, 2007.

Space Environment In-Situ Suite (SEISS) Performance and Operational Requirements Document (PORD), 417-R-SEISSPORD-0030, Baseline Version 2.0, November 16, 2005.

1.5 Revision History

Revision Number	Date	Author	Revision Description	Reason for Revision
1.0	Nov 6, 2009	Juan V. Rodriguez	Initial release	Initial release

2.0 OBSERVING SYSTEM OVERVIEW

2.1 Product Generated

The SEISS Differential-to-Integral flux algorithm produces integral proton flux values above a set of threshold energies from the 5-minute-averaged proton differential flux input, which in turn is based on the Level 1b corrected differential proton flux data. It also estimates the values of the differential flux at each of the threshold energies. These values are used to describe characteristics of the measured proton populations for scientific and operational purposes.

The SWPC Space Weather Forecast Office uses GOES integral proton fluxes for numerous operational alerts and radiation storm warnings. Therefore, NWS customers and forecasters require that the GOES-R Differential-to-Integral flux algorithm provide data continuity with the current GOES integral proton fluxes in order to avoid potential difficulties in interpretation. To this end, the GOES-R algorithm preserves the basic approach of the previous operational algorithm [Zwickl, 1989] that calculates integral proton fluxes from the Energetic Particle Sensor (EPS) on the GOES 8-12 (I-M) series and the Energetic Proton, Electron and Alpha Detector (EPEAD) on the GOES 13, 14 and P satellites. (Throughout this ATBD, the previous algorithm and measurements are referred to generically as “GOES I-P”).

2.2 Instrument Characteristics

The SEISS operational requirements and characteristics are detailed in section 3.3.6.1 of the GOES-R Series Mission Requirements Document (MRD, P417-R-MRD-0070) and the SEISS Performance and Operational Requirements Document (PORD, 417-R-SEISSPORD-0030). The requirements pertaining specifically to solar and galactic protons, which are pertinent to the integral flux algorithm, are in section 3.3.6.1.4 of the MRD and 3.2.3 of the PORD.

SEISS is a suite of three particle sensors: a magnetospheric particle sensor (MPS), a solar and galactic proton sensor (SGPS), and an energetic heavy ion sensor (EHIS). The SGPS measures proton fluxes in ten evenly spaced logarithmic energy bands from 1 MeV to 500 MeV and in an integral band above 500 MeV. It has two 90 degree FOVs, one looking west and the other looking east, as with the GOES N-P EPEAD. The westward FOV is the primary FOV for

alerts and warnings, for reasons described below. Having two FOVs provides redundancy as well as a westward view regardless of spacecraft yaw flip status.

The accuracy of the algorithm relies on precise instrument calibration and timing. Accurate calibration is critical as errors flow through to the 1- and 5-minute averaged differential flux output, used as input to the algorithm. The product's 25% accuracy requirement refers to the ground calibration accuracy requirement for the SEISS SGPS, including the contributions of Monte Carlo analysis to the calibrations.

Algorithm development by the Space Weather Algorithm Team assumes that the instrument meets the performance requirements outlined in the GOES-R MRD and SEISS PORD. In particular, it assumes that the response to out-of-band particles (including direction, energy range, and species) in any channel is no greater than 10% of the response to in-band particles, as specified by the PORD (3.2.1.5), after Level 1b processing. The out-of-band particles include the energetic cosmic ray background as well as electrons and out-of-band protons.

3.0 ALGORITHM DESCRIPTION

3.1 Algorithm Overview

The fundamental physical assumption of this algorithm is that the differential directional energy spectrum of solar protons above 1 MeV follows a power law in kinetic energy, with an exponent that in general varies with energy. This assumption is well supported by observations of solar and magnetospheric protons with energies in the 100's of keV to MeV range [e.g., Baker et al., 1979; Lario and Decker, 2002]. The algorithm converts the averaged, corrected SGPS differential proton flux measurements to integral fluxes using a piecewise power law determined from pairs of adjacent channels. The piecewise power law is used to interpolate on and integrate the measured differential flux spectrum in order to derive the integral flux above a given proton energy threshold. Estimates of the differential flux at the energy thresholds, which are byproducts of the integral flux calculation, are also output.

The algorithm provides basic exception handling (to handle missing flux values). It also sets limits and defaults on the value of the power law negative exponent, γ, in order to avoid using unrealistically extreme or noise-sensitive values of this parameter. In either case, a flag is set. Since γ is solved iteratively, the algorithm places a limit on the number of iterations. Flags are set when defaults are set, limits are reached or input data are missing.

3.2 Processing Outline

1. Read 5-minute average proton differential flux.
2. Estimate spectral exponent and flux coefficient for each differential channel pair, via an iterative solution for the energies that correspond to the input differential flux levels.
3. Calculate contribution of each sub-interval (based on differential channel energy ranges).
4. Sum sub-intervals above reference energy to obtain integral flux.
5. Save differential flux at reference energy as byproduct of the integration.
6. Set exception handling flags as needed.

3.3 Algorithm Input

The inputs to the algorithm consist of the 5-minute averages of SGPS L1b data, and ancillary data describing the energy resolution and geometrical factors of the individual SGPS proton channels.

3.3.1 Primary Sensor Data

The integral flux calculation requires 5 minute averaged proton differential flux input (SEISS.16). Averaging data reduces the effect of random measurement errors and allows quality flags to be assigned to the time period based on data gaps and number of averaged points in the time interval. A boxcar average without overlaps is a simple, well-understood method for calculating an average, and has been used for all previous GOES satellite particle flux averages. For SGPS, all proton flux measurements falling within a 5-minute window are given equal statistical weight in the average. That average is assigned to be representative of a single time point within the window. In typical boxcar averaging, the central time point of the window is selected. In previous GOES flux calculations, the earliest edge of the window has been used. This convention is being continued with the GOES-R particle measurements. For intervals where the measurements are uniformly distributed in time, this simple averaging technique provides an easily calculated and understood representation of the particle flux at a particular time.

The quantities assumed to be contained in the 5-minute averages of the SGPS L1b data (for one of the two SGPS FOVs) are defined in Table 1. The input files for both SGPS FOVs (+X and –X) have similar contents. The Differential-to-Integral Flux L2 product is calculated separately for the two SGPS FOVs.

In specifying the FOV center direction relative to the ENP coordinate system, it is assumed that the spacecraft axes are aligned to this coordinate system (where N is the normal to the orbital plane and E is directed toward the Earth along this plane). Given the large SGPS FOVs, this is not a critical assumption for small (~1 deg) differences between the spacecraft and ENP axes. The FOV center direction is a pass-through to the L2 product; it does not affect the L2 processing otherwise.

Based on current (September 2009) information available from the GOES-R program office, it is assumed that there is at least one “quality factor” recorded for each SGPS channel in the L1b data, and that this factor is the total correction applied to the fluxes for out-of-band / out-of-field contamination and backgrounds. Using the geometrical factors provided in the ancillary data (see

the next section), this quality factor can be used along with the corrected fluxes to get back to the original (averaged) uncorrected count rates. These quality factors are important quantities for the current algorithm since the uncorrected count rates are used to determine whether the exponential factor gamma (γ) should be set to its default.

SEISS L1b metadata have not been defined yet. Table 2 lists potential SEISS metadata that could be passed through to the L2 integral flux data records in future versions. The Differential-to-Integral Flux algorithm team has recommended to the GOES R program office that these metadata be included in the L1b records.

Table 1. L1b (5-minute-averaged) inputs to SEISS Differential-to-Integral Flux algorithm for a single SGPS FOV (east or west).

Averaged L1b Quantity	Sampling	Number of Values	Units	Purpose in L2 Calculations
Calibrated corrected differential proton fluxes	5 min ave	10 channels (1-500 MeV)	protons / (cm^2 s sr MeV)	Supports integral flux calculation
Calibrated corrected integral proton fluxes	5 min ave	1 channel (>500 MeV)	protons / (cm^2 s sr)	Not currently used by L2 algorithm; needed for cal / val
FOV Center Direction	5 min ave	3 cosines	Direction cosines in Local Spacecraft (ENP) coordinates	Identify West vs. East data
Total flux correction applied (out of band and background) to differential channels	5 min ave	10 channels (1-500 MeV)	protons / (cm^2 s sr MeV)	Determine threshold for default gamma; counting statistics for product uncertainties (cal/val)
Total flux correction applied (out of band and background) to integral channel	5 min ave	1 channel (>500 MeV)	protons / (cm^2 s sr)	Not currently used by L2 algorithm; needed for cal / val
Time	5 min	1 (start of period)	Julian date	Time stamp

Table 2. Potential SEISS SGPS L1b metadata to be considered for pass through to the L2 integral flux data records in future versions.

Metadata	Description
Spacecraft ID	GOES R satellite source
Instrument ID	EHIS, SGPS, MPS-Hi, or MPS-Lo, and serial number
Satellite position flag	Operating status and position (East, West, storage, transit, etc.)
Satellite location	Coordinates of satellite in earth-centered inertial (ECI) coordinates
Spacecraft yaw flip state	Status of yaw flip - no, yes, or during
L1b algorithm version number	L1b algorithm version number
Calibration table version	Version of table containing geometrical factors and channel energies.

3.3.2 Ancillary Data

Ancillary data are assumed to be data that are not generated on-orbit by SEISS or the spacecraft. The ancillary data required by the SEISS Differential-to-Integral Flux algorithm consist of characteristics of the SGPS channels. These characteristics consist of their upper and lower energies and their geometrical factors (Table 3). Uncertainties in these characteristics, as well as secondary (out-of-band) geometrical factors (or, equivalently, complete bandpass shapes), and FOV shapes, are identified as data required for cal/val activities, though not currently needed by the algorithm (Table 4). These data are products of the characterization of the SGPS in ground test and analysis.

In the past, the responses of individual flight models of the predecessor instruments (EPS and EPEAD) have been adjusted so that the same geometrical factors apply to all flight models. However, on-orbit comparisons of fluxes measured by different satellites, as well as comparisons of the east and west SGPS measurements at the time of a yaw flip, may reveal discrepancies sufficiently large that they should be removed in ground processing. Therefore, the processing architecture should sufficiently flexible to apply such empirical corrections to the geometrical factors for all look directions and channel energiews. This should be accomplished by defining flight-model-specific correction coefficients (primarily arising from cal/val) that can be applied to a common set of geometrical factors.

Table 3. Ancillary data related to SGPS performance characteristics required by the SEISS L2 Differential-to-Integral Flux algorithm.

Quantity	Refresh	Number of Values	Units	Purpose in L2 Algo-rithm	Source
Differential channel energy boundaries	Static	40: 2 boundaries for each of 10 differential channels for each (East and West) telescope	MeV	Calculate band centers	Ground calibration and analysis
Differential channel geometrical factors (primary)	Static; may change after cal/val or IFCs	20: 1 geometrical factor for each of 10 differential channels for each (East and West) telescope	cm^2 sr MeV	Determine threshold for default gamma	Ground calibration and analysis; on-orbit cal/val; IFCs

Table 4. Additional ancillary data related to SGPS performance characteristics that are needed for L2 cal/val.

Quantity	Refresh	Units	Purpose in L2 Cal/Val	Source
Differential channel energy boundary uncertainties	Static	MeV	Contribute to determining L2 product uncertainties	Ground calibration and analysis
Integral (>500 MeV) channel energy threshold and uncertainty	Static	MeV	Contribute to determining L2 product uncertainties	Ground calibration and analysis
Integral channel geometrical factor	Static; may change after cal/val	cm^2 sr	Contribute to determining L2 product uncertainties	Ground calibration and analysis
Channel secondary geometrical factors (or complete bandpass functions)	Static; may change after cal/val	cm^2 sr MeV (or cm^2 sr vs. energy)	Contribute to determining L2 product uncertainties	Ground calibration and analysis

Uncertainties of primary and secondary geometrical factors	Static	cm^2 sr MeV or cm^2 sr	Contribute to determining L2 product uncertainties	Ground calibration and analysis
FOV Shapes (Effective Area vs. Angle) and uncertainties	Static	cm^2 vs. angle	Intersatellite comparisons	Ground calibration and analysis

3.4 Theoretical Description

3.4.1 Physics of the Problem

Integral flux is a specification of the total directional flux of particles above an effective energy threshold. This algorithm reflects the calculation of this value for protons based on the energy spectrum of the measured differential flux. Differential flux is expressed in units of protons / (cm^2 s sr MeV). Integral flux is expressed in units of protons / (cm^2 s sr), a quantity also referred to as a particle flux unit (pfu). The threshold energies used in this algorithm are 1, 5, 10, 30, 50, 60 and 100 MeV, as in the GOES I-P algorithms. SWPC identifies the start of a solar proton event as the first of three consecutive 5 minute averages of the >10 MeV integral flux that are greater than or equal to 10 pfu, and issues an S1 alert. Higher levels of alerts are issued when the >10 MeV integral flux exceeds 100 (S2), 1000 (S3), 10,000 (S4), and 100,000 (S5) pfu. An alert is also issued when the >100 MeV integral flux exceeds 1 pfu, which is a better indicator of radiation risk to aircraft passenger and crews at high latitudes than the >10 MeV alerts. (See http://www.swpc.noaa.gov/ alerts/ description.html#proton.) The input GOES R L1b data have a 1 minute latency requirement due to the rapidity with which an SEP event can reach its peak level after triggering the initial alert.

The greatest geosynchronous proton fluxes above 1 MeV are observed during solar energetic particle (SEP) events. These energetic protons (as well as electrons and heavy ions) are believed to originate in shocks and magnetic field reconnections associated with coronal mass ejections (CME) [Cane and Lario, 2006]. The measurement of integral proton fluxes at geosynchronous orbit has both operational and scientific applications. These fluxes are sufficiently energetic to impact satellites in the region, causing undesired transient responses and single-event upsets and permanent damage in solid state devices and solar arrays, and the thresholds can be related to levels of shielding [Baker, 1996; O'Brien, 2009]. The proton fluxes also support alerts and warnings of radiation hazards to occupants of manned spacecraft and polar-crossing aircraft [Baker, 1996] and serve as inputs to operational predictions of *D* region

absorption of high-frequency and very-high-frequency (HF/VHF) radio waves [Sauer and Wilkinson, 2008].

The calculation of integral flux requires assumptions about the differential flux spectrum to be made. If a single statistical representation of the spectrum can adequately fit the data, the calculation requires only a simple fit to the data and the closed-form result of the integration of that fit above the reference energy. For example, a simple differential flux representation defined by two parameters, a single power law exponent and a reference-energy flux coefficient

$$j_i = j_0 E_i^{-\gamma}$$

appears as a straight line on a log flux vs log energy plot (Figure 1). This would imply that a simple linear fit is sufficient.

In general, however, the spectrum of solar energetic protons is not represented adequately by a single power law. The onset of a SEP event is a very important case (Figure 2), in which the highest energies arrive first (within tens of minutes of the acceleration of the source population to MeV energies). During such a period, when the data clearly exhibit velocity dispersion, the quantity γ varies piecewise from negative to positive in a single energy spectrum.

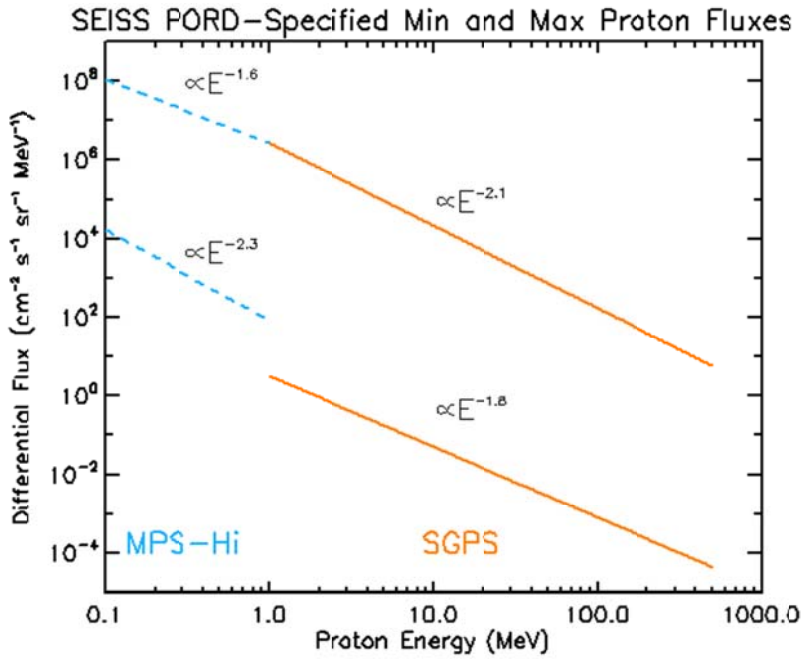

Figure 1. Minimum and maximum proton spectra specified in SEISS PORD for MPS-Hi and SGPS.

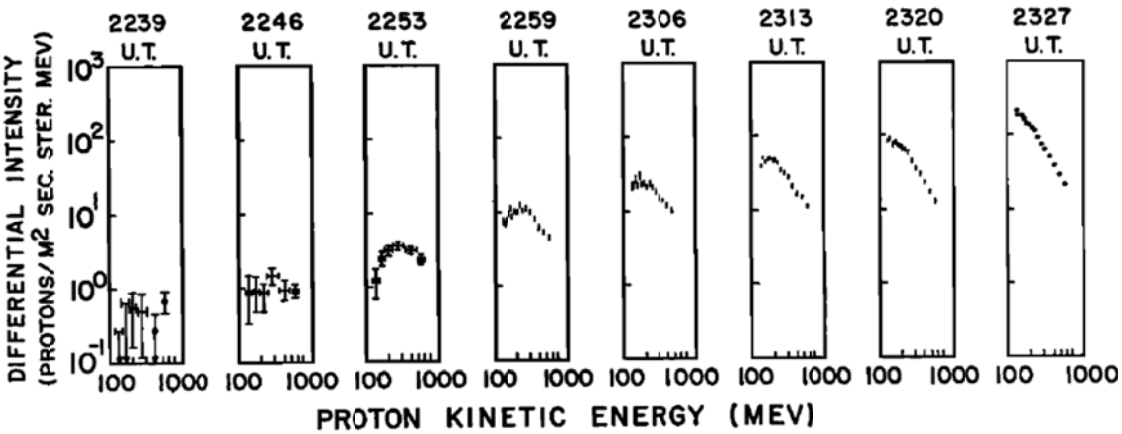

Figure 2. Rapid evolution of the 100-600 MeV spectrum of solar protons at 7-minute intervals during the onset of the SEP event of September 28, 1961, as measured by Explorer 12 [after Bryant et al., 1962, Figure 11].

Therefore, for spectra that are not adequately represented by a single power law distribution, as is often the case during times of interest, it is best to base the calculation on a method that is not limited by this assumption. We select a

method that is a modification of a simple trapezoidal summation commonly used for integral estimation. This allows us to limit the assumptions made about the shape of the spectrum to only the points where we have no data.

3.4.2 Mathematical Description

In order to estimate the integral of a function, a summing method can be used. Instead of doing the integration explicitly, the range is segmented into sub-ranges (see Figure 3) where the area under the curve can be well-represented by a single power-law functional form. These pieces of smaller area are then summed to provide the total integral. This estimation becomes better as the sub-ranges are made smaller.

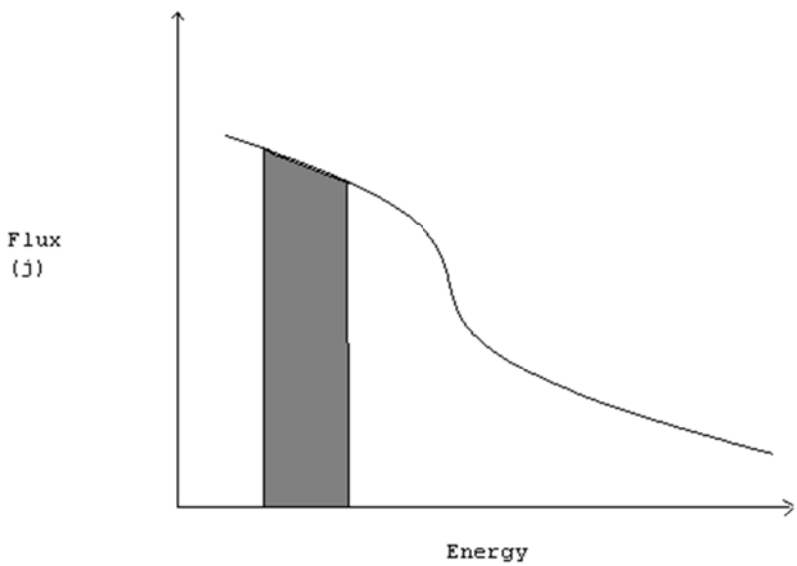

Figure 3. Description of a subsection of the integral flux spectrum

The sub-ranges in this calculation are defined by the energies of the SGPS differential flux measurements, and therefore cannot be made narrower to more accurately represent the integral. The SEISS SGPS solar proton measurements are made in channels that are rather wide in comparison to the energy dependence of the differential flux spectrum, though generally narrower than in the predecessor EPS and EPEAD detectors. However, we know that the

spectrum between the measurement values is not likely to be linear, and we can improve the estimation by applying the appropriate functional form to the curve between measurements. At these energies, a power law is a physically acceptable model of the differential flux spectrum that has been used extensively in legacy algorithms.

One approach is to recognize that the flux *J* integrated over an individual channel (i.e., the actual measured quantity) can be related to the differential flux at the channel edges

$$j_l = j_0 E_l^{-\gamma}$$
$$j_u = j_0 E_u^{-\gamma}$$

and to the measured count rate as follows:

$$J = \frac{C}{G} = \frac{j_0}{-\gamma+1}\left(E_u^{-\gamma+1} - E_l^{-\gamma+1}\right)$$

where *J* is the integral channel flux in protons / (cm^2 s sr), C is the corrected count rate, G is the geometrical factor (cm^2 sr), E_l and E_u are the lower and upper energies of the channel (MeV), γ is the negative power law exponent, and j_0 is the differential flux in protons / (cm^2 s sr MeV) at a reference energy (usually 1 MeV) [Armstrong, 1972, 1976; Zwickl, 1989]. Assuming the power law is constant across the channel, the differential flux at the midpoint E_m of the channel pass band (or at any other energy in the pass band) can be expressed as follows [Armstrong, 1976; Zwickl, 1989]:

$$j(E_m) = j_0 E_m^{-\gamma} = \frac{C(-\gamma+1)E_m^{-\gamma}}{G\left(E_u^{-\gamma+1} - E_l^{-\gamma+1}\right)}$$

In the latter expression, all of the quantities are known except γ. Therefore, γ has to be determined from a separate analysis. This was accomplished by Armstrong [1972, 1976] and Zwickl [1989] by tabulating γ as functions of ratios of corrected counts in adjacent channels and fitting the following expression to these tables over various ranges of validity:

$$\gamma = a + b \ln\left(\frac{C_i}{C_{i+1}}\right)$$

This approach is similar to the use of radiative transfer look-up tables in remote sensing algorithms. It has the virtue of avoiding the assumption of a channel center energy, which, if it is to have a physical meaning, depends on γ. The practical drawback of this approach is that it requires the generation of the look-up table (and subsequently the fits, if so desired). This is a major additional task that cannot be performed until the flight unit has been built and characterized and a sensor model created.

A second approach is taken by the GOES-R Differential-to-Integral Flux algorithm. This is driven by and takes advantage of the fact that the SEISS L1b differential channel data are expressed in terms of corrected differential fluxes at some set of energies identified as the channel centers, rather than in terms of counts per second. This approach avoids the determination of γ using fits to tables. However, it requires an iterative solution for the channel center energy and γ.

For each pair of differential channels (i, $i+1$), we have the 5-minute averages of the L1b corrected differential fluxes (j_i) and the lower and upper channel passband energies $E_{i,l}$ and $E_{i,u}$, for i = 1, 2, …, 10. The passband energies are ancillary data and are determined during instrument characterization.

In this analysis, the channel center energy E_i is taken to be the energy at which the quantity

$$j_i = \frac{C_i}{G_i\left(E_{u,i} - E_{l,i}\right)}$$

is equal to the differential flux. The initial guess for each channel center energy is calculated as the geometric mean of the lower and upper channel passband energies:

$$E_i = \sqrt{E_{i,l} E_{i,u}}$$

This is only an initial guess – the mean energy of the measured flux depends in general on the channel energy response as well as the actual differential flux spectrum – but it is preferable to a linear average for a power law with $\gamma > 0$. Assuming a power law, the differential number flux at two adjacent band center energies is expressed as:

$$j_i = j_{0,i} E_i^{-\gamma_i}$$

$$j_{i+1} = j_{0,i} E_{i+1}^{-\gamma_i}$$

From these two equations, the gamma parameter γ_i and the reference-energy differential flux $j_{0,i}$ are obtained for each subinterval:

$$\gamma_i = \frac{\ln\left(\frac{j_{i+1}}{j_i}\right)}{\ln\left(\frac{E_i}{E_{i+1}}\right)}$$

$$j_{0,i} = j_i E_i^{+\gamma_i}$$

Note that $j_{0,i}$ has the same units as differential flux.

The iterative solution for the channel center energy E_i and γ_i (and therefore $j_{0,i}$) relies on analytical expressions for E_i as a function of γ_i and the channel edge energies. Assuming a power law, it can be shown that the energy E_i at which the quantity

$$j_i = \frac{C_i}{G_i\left(E_{u,i} - E_{l,i}\right)}$$

is equal to the differential flux is given by

$$E_i = \left[\frac{(-\gamma+1)(E_u - E_l)}{\left(E_u^{-\gamma+1} - E_l^{-\gamma+1}\right)}\right]^{\frac{1}{\gamma}}$$

for $\gamma \neq 0$ or $\gamma \neq 1$. If $\gamma = 1$, then the expression is

$$E_i = \frac{(E_u - E_l)}{\ln\left(\frac{E_u}{E_l}\right)}$$

If $\gamma = 0$, then the above expression for j_i is correct at all energies in the band, and absent a unique answer for E_i, the average energy can be used. Note that these analytical expressions have been derived under the assumption that the channel response is flat between E_l and E_u and zero outside these energies. This is consistent with the approach of a single, band-integrated geometrical factor for each channel used by Zwickl [1989] and in the present algorithm.

The iterative solution proceeds as follows:

1. Estimate the set of γ_i and $j_{0,i}$ using the geometric mean of the channel edge energies for E_i.
2. Use these estimates for γ_i to estimate a new set of E_i using the analytical expressions derived above.
3. Since there are two γ's associated with each channel (except for the lowest and highest energy channels), one below the center energy and one above the center energy, there are two new E_i's for each channel. In this case, linearly average the two estimates to derive the new estimate of E_i going forward.
4. Calculate new estimates of γ_i from the new set of E_i.
5. Set a γ_i to the default value if the input corrected counts in the lower energy channel of a given pair are less than the standard deviation of the running average of the background counts (see below).
6. If a new estimate of γ_i falls outside of the range of reasonable values (±8), set it to the nearest (upper or lower) limit of +8 or -8 [Zwickl, 1989].
7. If, for a given channel, the new E_i estimate is different by less than 1% than the previous estimate of E_i, then stop the iteration, otherwise repeat 2-4.
8. If, after ten iterations (ten occurrences of steps 2-4), the value of E_i is still changing by more than 1%, then stop the iteration, report the initial guess of E_i and γ_i and set the flag isNotConverged to 1.
9. Calculate the set of $j_{0,I}$ from the final set of E_i and γ_i.

The integral flux for each subinterval, $J_{i->i+1}$, is calculated using the obtained value of gamma, and the average (or representative) energy of the channel.

$$J_{i\to i+1} = \int_{E_i}^{E_{i+1}} j_{0,i} E_i^{-\gamma_i} dE$$

$$J_{i\to i+1} = \frac{j_{0,i}}{-\gamma_i + 1}\left(E_{i+1}^{-\gamma_i+1} - E_i^{-\gamma_i+1}\right)$$

The total integral flux, J, is then obtained by summing the area of each subinterval with energies above the specified reference energy. The lowest energy contribution to the integral flux, between the threshold energy and the next channel center energy E_{i+1}, is calculated either by interpolation or extrapolation, as follows.

If the threshold energy $E_{L,k}$ is greater than the geometric-mean (initial guess) center energy E_i of channel i but less than the upper boundary energy $E_{u,i}$ of channel i, then the contribution between the threshold energy and the iterated center energy of the next channel E_{i+1} is calculated as an interpolation using γ_i and $j_{0,i}$:

$$J_{L,k\to i+1} = \frac{j_{0,i}}{-\gamma_i + 1}\left(E_{i+1}^{-\gamma_i+1} - E_{L,k}^{-\gamma_i+1}\right)$$

The differential flux is also calculated and reported at the threshold energies:

$$j_{L,k} = j_{0,i} E_{L,k}^{-\gamma_i}$$

Given the expected SGPS energy channels, these expressions are used for the >5, >10, and >60 MeV integral fluxes and the 5, 10 and 60 MeV differential fluxes.

If the threshold energy $E_{L,k}$ is greater than the lower boundary energy $E_{l,i+1}$ of channel i+1 but less than the geometric-mean (initial guess) center energy E_{i+1} of channel i+1, then the contribution between the threshold energy and the iterated

center energy of the next channel E_{i+1} is calculated as an extrapolation using γ_{i+1} and $j_{0,i+1}$:

$$J_{L,k\to i+1} = \frac{j_{0,i+1}}{-\gamma_{i+1}+1}\left(E_{i+1}^{-\gamma_{i+1}+1} - E_{L,k}^{-\gamma_{i+1}+1}\right)$$

The differential flux is also calculated and reported at the threshold energies:

$$j_{L,k} = j_{0,i+1}E_{L,k}^{-\gamma_{i+1}}$$

Given the expected SGPS energy channels, this expression is used for the >1, >30, >50, and >100 MeV integral fluxes and the 1, 15, 30, 50 and 100 MeV differential fluxes. This amounts to a small extrapolation downwards in energy that should be more representative of the fluxes in question. In principle, this prevents signatures of magnetospheric processes in the lowest two channels from being included in the >5 MeV integral fluxes, though in practice this is not a concern with the expected SGPS channels, where the 5 MeV threshold lies above the center energy of P3 (4.6 MeV). The choice of interpolation vs. extrapolation is set in the code by a table that needs to be tailored to the final characterized SGPS channel energies as well as any variation among flight units.

Finally, the integral flux is calculated as a sum of the segment integral fluxes:

$$J_{>E_{L,k}} = J_{L,k\to i_{\min}} + \sum_{i=i_{\min}}^{9} J_{i\to i+1}$$

Note that P11, the SGPS >500 MeV integral flux channel, is not included in the sum since the GOES I-P EPS/EPEAD instruments do not include such a channel. If it were included, the integral flux between E_{10} (371 MeV) and 500 MeV would also have to be calculated and included in the sum. Given typically large γ values at these energies, this omission does not have a significant effect on the calculation of the >100 MeV fluxes.

The power law expression implicitly assumes that the energy is normalized to some reference energy such that $j_{0,i}$ is the flux at this energy and the term $E^{-\gamma}$ is a unitless shape function. For the solar proton integral fluxes, the natural reference energy is 1 MeV, the differential flux is in units of protons cm^{-2} s^{-1} sr^{-1} MeV^{-1}, and

the channel energies are expressed in MeV. If the reference energy were chosen to be 1 keV, as in the SEISS PORD, then the channel energies would be expressed in keV, and $j_{0,i}$ would be in units of protons cm^{-2} s^{-1} sr^{-1} keV^{-1} and would be scaled by the variation of the spectrum in question from 1 MeV to 1 keV. For example, the maximum solar proton spectrum specified by the SEISS PORD (Figure 1) in terms of proton energies in keV

$$j = 5.4 \times 10^9 E^{-2.1} \text{ cm}^{-2} \text{ s}^{-1} \text{ sr}^{-1} \text{ keV}^{-1}$$

is equivalent to

$$j = 2.7 \times 10^6 E^{-2.1} \text{ cm}^{-2} \text{ s}^{-1} \text{ sr}^{-1} \text{ MeV}^{-1}$$

if E is expressed instead in MeV.

Simulations show that the expression for $j_{0,i}$ that uses the channel center energy

$$j_{0,i} = j_i E_i^{+\gamma_i}$$

and the expression for $j_{0,i}$ used by Zwickl [1989] (termed $A_{i,i+1}$), which uses channel edge energies,

$$A_{i,i+1} = \frac{C_i(-\gamma_i + 1)}{G_i\left(E_{u,i}^{-\gamma_i+1} - E_{l,i}^{-\gamma_i+1}\right)}$$

give similar results if γ varies slowly over the interval and E_i and γ_i are solved iteratively.

In the absence of solar protons, the channels with energies less than approximately 5 MeV contain a trapped, magnetospheric population of energetic protons. In the interval that brackets this energy, γ is commonly determined from a pair of fluxes, the higher energy channel of which is close to or at instrument background levels. While the GOES I-P estimates of >1 MeV integral flux under trapped magnetospheric conditions depend on this single estimate of γ and $j_{0,i}$, the GOES R estimates benefit from at least two channels (P1 and P2) from which a reliable estimate of γ for the magnetospheric fluxes can be derived.

3.4.3 Considerations in the Presence of Background Counts

Special considerations must be made in calculating the contributions from each sub-interval during times of low count rate. During these times, the measurements may be in the noise level, and the calculation of γ and j_0 could be greatly affected by small variations in the background count, and not representative of the actual population. When, in any given channel pair, the corrected count level in the lower energy channel drops below the standard deviation of a running average of the uncorrected background counts in that channel, an average value of γ is assumed [Zwickl, 1989].

For each channel, the corrected fluxes j_i^c and the flux correction Δj_i^c (both assumed to be in flux units and averaged over 5 minutes) are multiplied by the characterized, channel-integrated geometrical factor $G\Delta E$ to retrieve the equivalent counts per second C_i^C and ΔC_i (see Table 5 for the GOES-7 values of $G\Delta E$ used in processing GOES I-P data). The uncorrected count rate C_i^U in each channel is then determined by adding the corrected count rate and the count rate correction:

$$C_i^C = G_i \Delta E_i \; j_i^C$$
$$C_i^U = G_i \Delta E_i \left(j_i^C + \Delta j_i \right)$$

The uncorrected count rate C_i^U is then compared to the upper limits to the background count rates listed in Table 5 or Table 6. If the uncorrected count rate is less than this limit in a given channel, then the current record is identified as being dominated by background counts, and it is assessed further.

The standard deviation of the uncorrected counts is calculated from a 4-hour (48 samples x 5 minutes/sample) running average of the uncorrected *background* count rate (τ is the current time index):

$$\overline{C_i^U}(\tau) = \overline{C_i^U}(\tau - 1) + \left[C_i^U(\tau) - \overline{C_i^U}(\tau - 1) \right] / 48.0$$

This is similar to the running average of the background count rate currently calculated in the GOES I-P algorithm for determining the minimum background count rate in a 10-day period. By using the running average, we prevent

fluctuations in the uncorrected background count rate from strongly influencing the determination of γ. The "seed" background count rate, given in Table 5, was determined from GOES-7 data measured on March 7 and 23, 1989 [Zwickl, 1989].

Table 5. Various GOES I-P constants used in determining and applying the background correction by the Zwickl [1989] algorithm.

GOES I-P EPS Channel i	Geometrical Factor $G_i \Delta E_i$ (cm^2 sr MeV)	Upper limits to backgrounds (counts/sec)	"Seed" count rate from GOES-7 (counts/sec)	γ_i default values
P1	0.202	0.200	0.06	1.3
P2	0.252	0.090	0.018	1.4
P3	0.325	0.070	0.01	1.5
P4	4.64	0.250	0.05	1.7
P5	15.5	0.800	0.10	1.9
P6	90.0	1.20	0.19	2.0
P7	300.0	2.50	0.29	--

Table 6. The quantities from Table 5, interpolated to the SGPS channels. Information on SGPS actual performance, including geometrical factors and background levels, is not generally available as of September 2009. These quantities will need to be reassessed when the SGPS performance is validated.

GOES R SGPS Channel i	Geometrical Factor $G_i \Delta E_i$ (cm^2 sr MeV)	Upper limits to backgrounds (counts/sec)	"Seed" count rate from GOES-7 (counts/sec)	γ_i default values
P1	0.050	0.050	0.060	1.3
P2	0.073	0.063	0.052	1.3
P3	0.185	0.105	0.032	1.3
P4	0.308	0.087	0.014	1.4
P5	1.30	0.138	0.027	1.6
P6	2.98	0.158	0.060	1.7
P7	14.4	0.744	0.100	1.9
P8	46.3	0.883	0.165	1.9
P9	97.5	0.949	0.260	2.0
P10	175.5	1.442	0.290	--

Using this running average of the count rate, the standard deviation of the uncorrected counts is calculated assuming Poisson counting statistics:

$$\sigma_i = \left(\overline{C_i^U} \Delta t\right)^{\frac{1}{2}}$$

where Δt is the 300-second averaging period. This standard deviation is then compared to the total corrected counts in the current period. If the following inequality is true for the lower energy channel in the channel pair (i, i+1) used to calculate a given γ_i:

$$C_i^C \Delta t < \sigma_i$$

then the default γ_i is used for the energy interval (i, i+1). See Table 5 for the default γ_i used in the GOES I-P algorithm.

3.4.4 Algorithm Output

The algorithm outputs a value of integral flux above the specified threshold energies (1, 5, 10, 30, 50, 60 and 100 MeV) for 5-minute averaged differential flux measurements. It also outputs an estimate of the differential fluxes at these energies plus 15 MeV (Table 7). The exception handling flags hasMissingFlux, isBackground, hasGammaLimit, and isNotConverged are also output by the algorithm. Currently it is not known whether the East and West fluxes and flags will be output in one record or in separate records. This depends on the L1b formats, which have not been defined as of September 2009.

Table 7. Level 2 Outputs of SEISS Differential-to-Integral Flux Algorithm.

Data Type	Refresh	Number of values	Units
Integral Proton Fluxes, West	5 min	At the 7 threshold proton energies	protons / (cm^2 s sr)
Integral Proton Fluxes, East	5 min	At the 7 threshold proton energies	protons / (cm^2 s sr)
Differential Proton Fluxes at Energy Thresholds, West	5 min	At the 7 threshold proton energies plus 15 MeV	protons / (cm^2 s sr MeV)
Differential Proton Fluxes at Energy Thresholds, East	5 min	At the 7 threshold proton energies plus 15 MeV	protons / (cm^2 s sr MeV)
hasMissingFlux, West	5 min	1	none

Data Type	Refresh	Number of values	Units
hasMissingFlux, East	5 min	1	none
isBackground, West	5 min	9	none
isBackground, East	5 min	9	none
hasGammaLimit, West	5 min	9	none
hasGammaLimit, East	5 min	9	none
isNotConverged, West	5 min	10	none
isNotConverged, East	5 min	10	none
Time	5 min	1 (start of period)	Julian date

4.0 TEST DATA SETS AND OUTPUTS

4.1 Simulated/Proxy Input Data Sets

The proton integral flux calculation requires input of 5-minute-averaged corrected differential flux values. Data sets are created for periods around the occurrence of a solar energetic particle (SEP) event (Table 8). These sets are intended to represent a wide range of conditions. Any given set encompasses an SEP event onset, peak, and decay, and the magnetospheric-only populations preceding or following it. Both westward and eastward observations are represented, the latter of which tend to exhibit more short-term fluctuations.

Table 8. Test Cases (SEP onsets and active region location from "Solar Proton Events Affecting the Earth Environment, January 1976 – July 2007," at http://www.swpc.noaa.gov/ftpdir/indices/SPE.txt)

SEP Event Onset (Day / UT)	Active Region Location	Period of Test Data (00 UT start/end times assumed)	Source Satellite / FOV Direction	Characteristic
2001 Sep 24 / 1215	S15E23	Sep 24 – Oct 3	GOES 8 (West) GOES 10 (East)	Two event onsets
2001 Nov 22 / 2320	S15W34	Nov 22 – Nov 30	GOES 8 (West) GOES 10 (East)	Short duration (~3 days) and highly variable E fluxes
2004 Jul 25 / 1855	N08W33	Jul 25 – Jul 30	GOES 11 (West) GOES 10 (East)	Two superposed events, highly variable E and W fluxes
2006 Dec 06 / 1555	S07E79	Dec 3 – Dec 9	GOES 11 (West GOES 10 (East)	Trapped particles followed by gradual event onset and peak

Proxy data are constructed from GOES 8, 10 and 11 EPS corrected differential proton flux measurements. Because the detector center energies are different, the measured proton fluxes are resampled to GOES-R SGPS energies using log-log interpolation (Figure 4). In order for the resampled fluxes to be accurate in the presence of large γ, the center energies must be determined iteratively before performing the interpolation. Then, the integral flux in each channel, calculated by integrating the resampled differential flux spectrum, is divided by the channel energy range in MeV to simulate the Level 1b differential fluxes expected by the algorithm. The proxy data include date and time, resampled differential flux and flux correction values, and direction cosines.

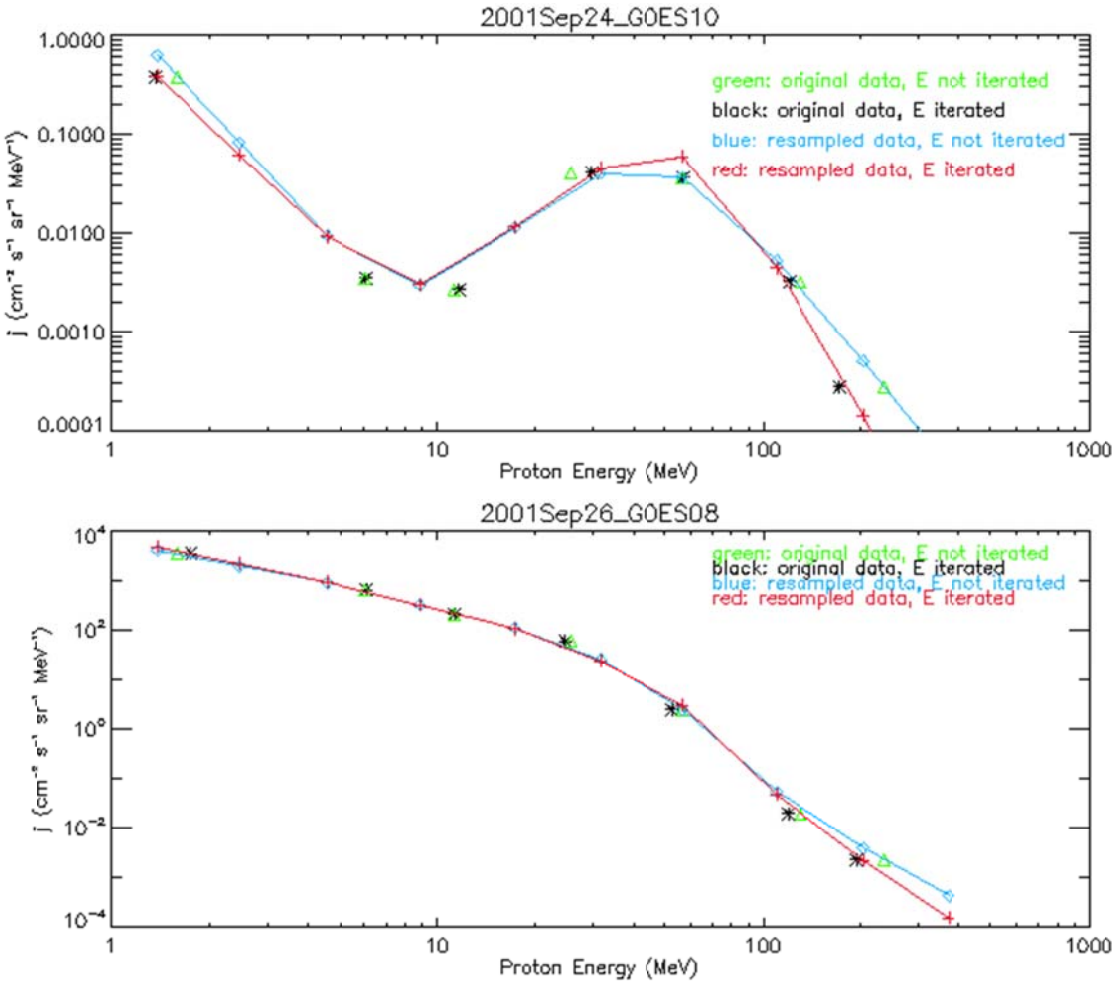

Figure 4. Comparison of GOES-R resampled proxy data with original GOES 8 and 10 data, for solar proton spectrum measured at 12 UT on September 24 and 26, 2001. The upper plot depicts a transitional spectrum from the onset of the SEP event, comprised of solar protons above 10 MeV and trapped magnetospheric protons below that. Without iterating on the center energies, the >1 MeV and >100 MeV integral fluxes in particular would be greatly overestimated due to the large γ. The lower plot depicts a spectrum following the peak of the SEP event, in which iterating on the center energies only improves the accuracy of the >100 MeV integral fluxes.

The central values and energy ranges for the GOES-R detector are summarized in Table 9. These are the values that are used for testing and validation of the integral flux algorithm. In addition, the energies of the GOES I-P channels are given in Table 10, for comparison.

Table 9. GOES-R SGPS proton channel energies used as initial guesses in L2 Algorithm.

GOES-R SGPS Channel	Lower energy of channel (MeV)	Upper energy of channel (MeV)	Central energy (geometrical mean) of channel (MeV)
P1	1.0	1.9	1.38
P2	1.9	3.2	2.47
P3	3.2	6.5	4.56
P4	6.5	12.0	8.83
P5	12.0	25.0	17.3
P6	25.0	40.0	31.6
P7	40.0	80.0	56.6
P8	80.0	150.0	109.5
P9	150.0	275.0	203.1
P10	275.0	500.0	370.8

Table 10. GOES I-P EPS/EPEAD proton channel energies as documented by Zwickl [1989] and used in the operational processing code.

GOES I-P EPS Channel	Lower energy of channel (MeV)	Upper energy of channel (MeV)	Central energy (geometric mean) of channel (MeV)
P1	0.6	4.2	1.6
P2	4.2	8.7	6.0
P3	8.7	14.5	11.2
P4	15.0	44.0	25.7
P5	39.0	82.0	56.6
P6	84.0	200	130
P7	110	500	235

The output of the GOES-R algorithm is compared with the archived GOES I-P integral flux channels for verification of the delivered L2 algorithm code performance. These proxy test results are documented in the SEISS Differential-to-Integral Flux Algorithm Test Plan and Results document.

The differences between the results of the Zwickl [1989] and GOES-R algorithms do not by themselves indicate whether one or the other is “better”, since the only “truth” we have are the seven “differential” channels of relatively low energy resolution from the GOES I-P measurements. It is expected that the improved

spectral sampling of SGPS relative to EPS and EPEAD will bring the GOES-R estimates closer to the "truth," but this cannot be shown with the proxy data since they are interpolated from the GOES I-P measurements.

Therefore, we have simulated "true" spectra using analytical fits to subsets of the test cases listed in Table 8 that contain SEP-level fluxes. Functional forms are chosen that adequately reproduce the spectral and temporal variability of the SEP differential fluxes. The "true" output differential and integral fluxes are calculated analytically from these forms. They provide a basis against which to compare the outputs of the GOES I-P algorithm and the GOES-R algorithm, the latter at both the GOES I-P and GOES-R sampling. Obviously, these fitted spectra cannot reproduce higher frequency variations in energy that are missed by the instrumental sampling considered here. However, they provide a valid albeit smoothed basis against which to compare the outputs of the two algorithms. These simulated results are documented below.

4.1.1 Trapped Proton Fluxes in the Lowest Channels

In the absence of solar protons, trapped magnetospheric protons (< 5 MeV) are measured by the GOES I-P EPS/EPEAD P1 channel. SGPS measures magnetospheric protons in channels P1-P3. Due to the coarse energy sampling by EPS of the > 0.6 MeV tail of the magnetospheric population, γ for this tail is determined from the counts in P1 and P2, the latter of which may be close to background levels and therefore noisy. Therefore, it should be considered whether the proxy data created for magnetospheric conditions for SGPS P1-P3 are representative of magnetospheric proton spectra. Two individual spectra from ATS-6 indicate $\gamma \sim 5$ and $\gamma \sim 6$ in the 0.3-1 MeV range [Fritz et al., 1977], while two individual substorm spectra have $\gamma = 5.12$ and $\gamma = 6.45$ in the 0.1-1 MeV range [Baker et al., 1979]. Therefore, if the γ determined from GOES I-P P1 and P2 fluxes (nominally 1.6-6.0 MeV central energies) outside of SEP events is between 5 and 7, the resampled proxy data are reasonable for testing the GOES-R Differential-to-Integral flux algorithm under magnetospheric conditions. This does not rule out the validity of other values of γ that may be derived.

4.2 Construction of Simulated Proton Spectra

For fitting the measured proton spectra, an exponential in energy (i.e., a Maxwellian) was originally considered by virtue of its simplicity. It lends itself to a

linear least-squares fitting of the logarithm of the fluxes vs. energy, and the integrals and derivatives are easy to calculate. However, Maxwellians generally roll off too rapidly at the high end to account for the spectra above ~130 MeV, and therefore do not provide an adequate test of the calculation of the >100 MeV integral fluxes. In addition, they cannot account for the separate component of trapped magnetospheric protons in P1.

To account properly for the highest energy channels, we have chosen to represent the solar protons with a kappa distribution [Vasyliunas, 1968]. A kappa distribution has three adjustable parameters: the number density *n*, the characteristic energy E_o, and the spectral parameter kappa (κ), which is identically γ at high energies. Kappa distributions have been used to describe magnetospheric particle populations as single distributions that are Maxwellian at low energies but have an enhanced (power-law) high-energy tail [Christon et al., 1988, and references therein]. We are not aware of the use of kappa distributions in describing solar proton spectra, but they are sufficient for our present purpose.

The differential flux corresponding to a kappa distribution is given by

$$j_\kappa(E) = \frac{nc}{(2m_p c^2)^{1/2} E_o^{3/2}} \frac{\Gamma(\kappa+1)}{(\pi\kappa)^{3/2}\Gamma\left(\kappa-\frac{1}{2}\right)} \frac{E}{\left(1+\frac{E}{\kappa E_o}\right)^{\kappa+1}}$$

and the integral flux is given by

$$J_\kappa(>E) = \frac{nc}{\pi^{3/2}} \left(\frac{\kappa E_o}{2m_p c^2}\right)^{1/2} \frac{\Gamma(\kappa-1)}{\Gamma\left(\kappa-\frac{1}{2}\right)} \frac{\left(1+\frac{E}{E_o}\right)}{\left(1+\frac{E}{\kappa E_o}\right)^{\kappa}}$$

where, in addition to the parameters defined above, *c* is the speed of light in free space, $m_p c^2$ is the rest mass of a proton in MeV, and Γ is the gamma function [Vasyliunas, 1968].

The lowest energy channel, P1, generally includes variations in the trapped magnetospheric population that are not reflected in the higher energy channels, and also generally has a different spectral index than the solar protons. Therefore, it is treated separately with a simple power law expression. The flux coefficient j_0 is the free parameter:

$$j_p(E) = j_0 E^{-5.5}$$

The spectral sampling of P1 and P2 in the GOES I-P data is inadequate to constrain the value of γ; therefore for this analysis we assume γ=5.5 based on the magnetospheric observations referenced above.

An example of a pair of westward (GOES 8) and eastward (GOES 10) observations of solar proton spectra during the SEP event that started on September 24, 2001, is shown in Figure 5. The results of the least-squares fits to a kappa function are shown with and without the inclusion of a power law component at the lowest energies to account for a separate magnetospheric trapped population. The results show that, in these cases, the parameters of the kappa distribution are not significantly affected by the inclusion of the power law component in the fit. The wide spectral spacing between the first and second channels (P1 and P2) illustrates how the EPS measurements cannot constrain the value of γ for the power law. The magnetospheric component in P1 is more prominent in the eastward-observed fluxes because in general the westward-observed solar proton fluxes are greater than the eastward-observed fluxes. Under these conditions, where the fluxes in P1 are significantly greater than the fluxes in P2, the fits incorporating this power law component are likely to be successful. Otherwise, if P1 is similar to or less than P2 during a large portion of an SEP event, then this approach is not satisfactory for the event. We found that, of the test cases used in this analysis, only the September 24, 2001 SEP event could be fit continuously throughout the event with the sum of a kappa distribution and power law. However, this one case is sufficient to simulate the effect of improved SGPS spectral sampling below 5 MeV on the integral and differential flux retrievals. For the other cases, we fit the measured spectra to a kappa function only, omitting P1 from the fit.

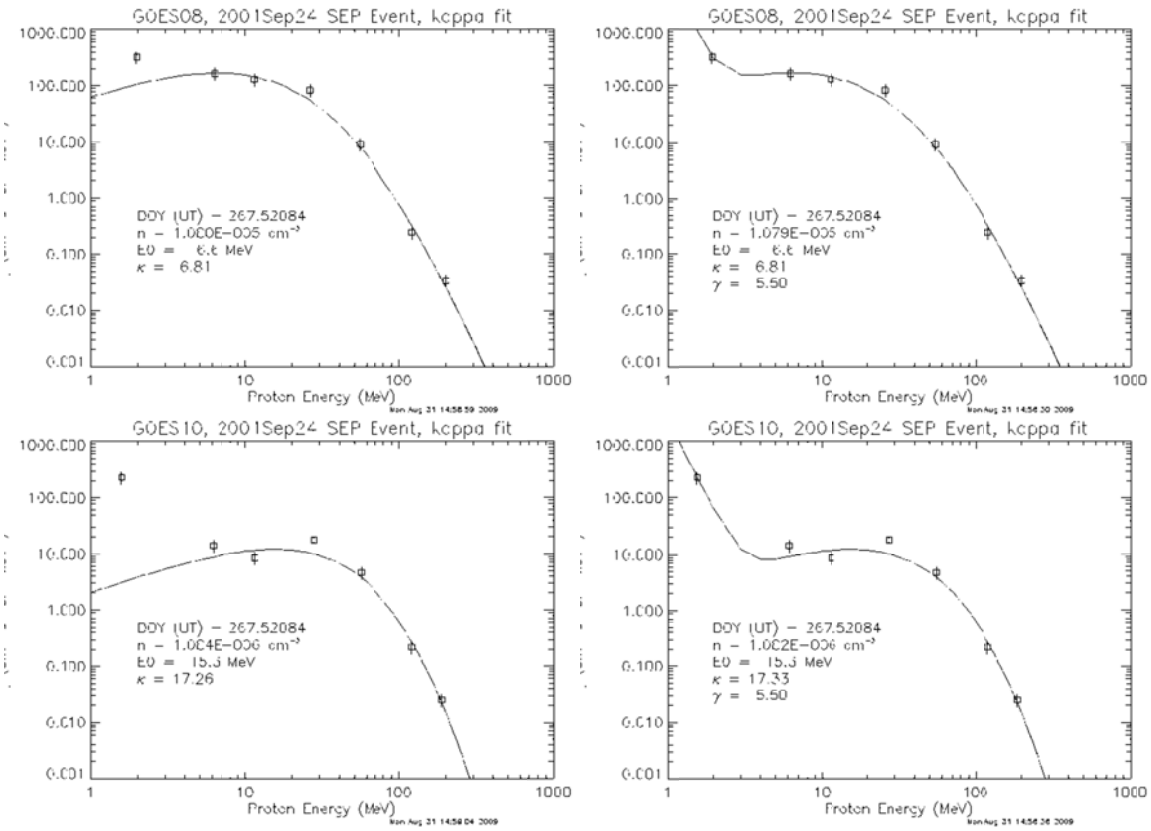

Figure 5. Comparison of GOES 8 (westward) and GOES 10 (eastward) observations of solar proton differential fluxes and least-squares fits to a kappa function without (left) and with (right) a power law component at the lowest energies with $\gamma = 5.5$.

The retrieval simulation with fitted spectra follows these steps:

1. Estimate the energies-at-fluxes for the differential input fluxes using the iterative technique from the algorithm
2. Fit the spectra with the adjusted energies to kappa distribution (or the sum of the power law and kappa distributions) using a Levenberg-Marquardt non-linear least squares fit [Press et al., 1988]. The fits are not calculated when the differential flux in the P2 channel is less than 1 proton / (cm^2 s sr MeV).
3. Calculate the “true” input channel fluxes and output differential and integral fluxes and the slopes using the fitted expression
4. Run the GOES I-P Zwickl [1989] algorithm on the “true” input channel fluxes for the GOES I-P channels
5. Run the GOES R algorithm on the “true” input channel fluxes for the GOES I-P and the GOES R channels, including the iteration on the energies-at-fluxes

6. Compare the results, calculating the RMS difference between each retrieval and the truth as a function of energy

4.3 Test Results Using Simulated Proton Spectra, including Uncertainty Estimates

Integral and differential flux retrievals from the simulations for the cases listed in Table 8 are plotted in Figure 6 through Figure 13. The retrievals were performed using IDL versions of the Zwickl [1989] and the GOES R algorithms. The background levels were not used to limit the values of gamma. In all cases, the inputs were channel-integrated “differential” fluxes derived from the “true” spectra based on the kappa distribution fits. The Zwickl [1989] algorithm ingested fluxes calculated at the GOES I-P EPS/EPEAD spectral sampling and resolution, while the GOES R algorithm processed data at both the EPS/EPEAD and the GOES R SGPS sampling and resolution. The event root-mean-squared (RMS) errors between the retrievals and the “truth” are summarized in Figure 14 and Figure 15. These are primarily systematic errors; no noise is introduced into the simulations.

Some of the salient results of this simulation are as follows:

1. Generally, the GOES R algorithm operating on the SGPS data performs better than the Zwickl [1989] algorithm or GOES R algorithm operating on the EPS/EPEAD data.
2. The event RMS errors with the new algorithm/instrument combination lie generally in the 1-10% range.
3. For the magnetospheric power law model used in the September 24, 2001 case, the improved SGPS spectral sampling below 5 MeV results in a reduction in the >1 MeV integral flux error from a ~100% overestimate to 1%.
4. The Zwickl [1989] algorithm tends to overestimate the >100 MeV integral flux, by as much as 100%. The error in the GOES R algorithm >100 MeV flux is 10% or smaller.
5. The 50 MeV differential flux retrievals are somewhat worse for the GOES R algorithm/instrument combination than for the other retrievals. However, the errors are generally 10% or less at this energy.

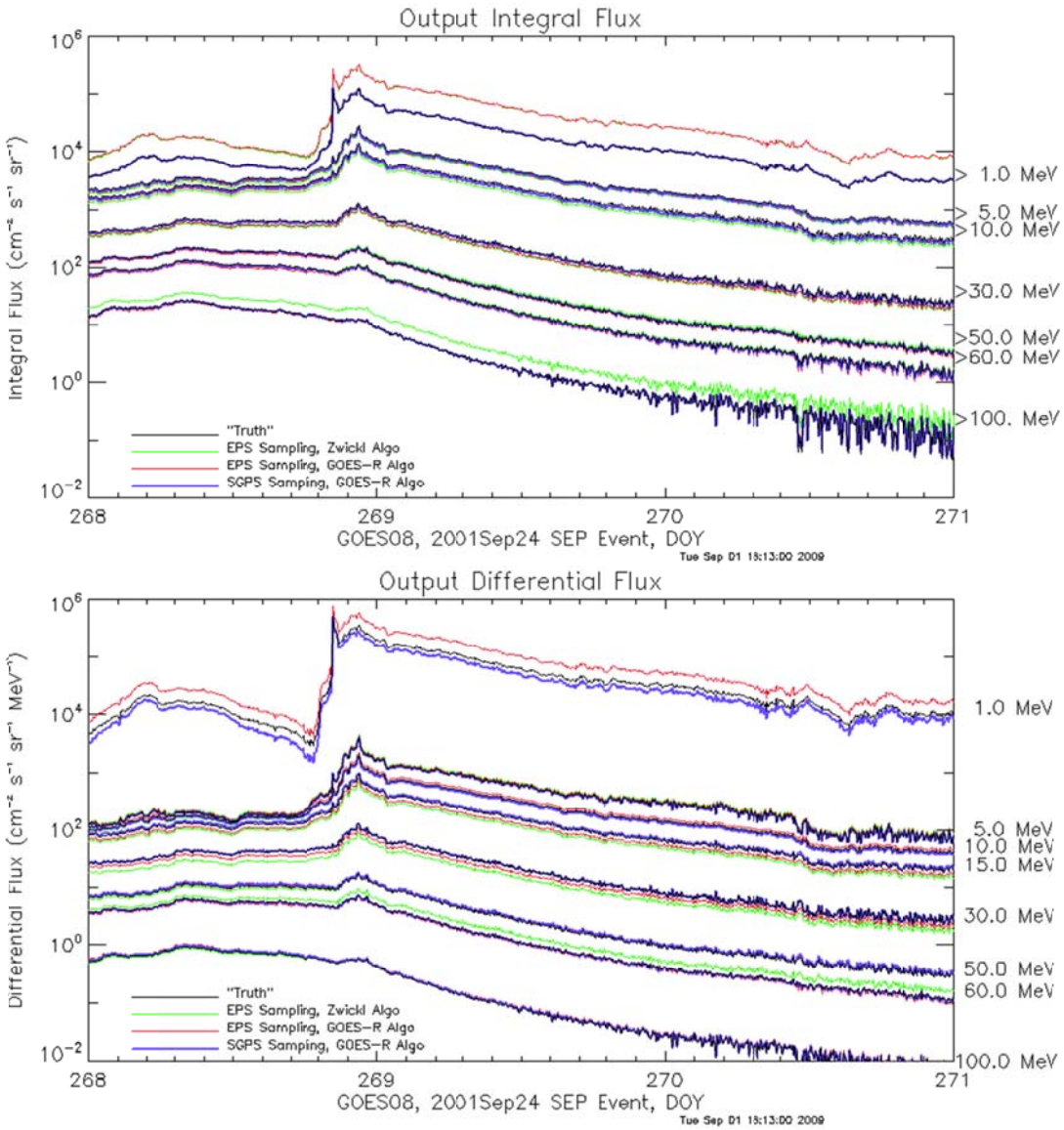

Figure 6. Comparison of integral flux and differential flux retrievals to "truth" for the GOES 8 westward observations of solar protons during the September 24, 2001 SEP event. The black curves represent the "truth" from fits to the GOES 8 data using a combined kappa distribution and power law. The green curves represent the retrievals by the Zwickl [1989] algorithm. The red curves represent the GOES R algorithm retrievals using data at the GOES I-P EPS/EPEAD spectral resolution. The blue curves represent the GOES R algorithm retrievals using data at the SGPS spectral resolution.

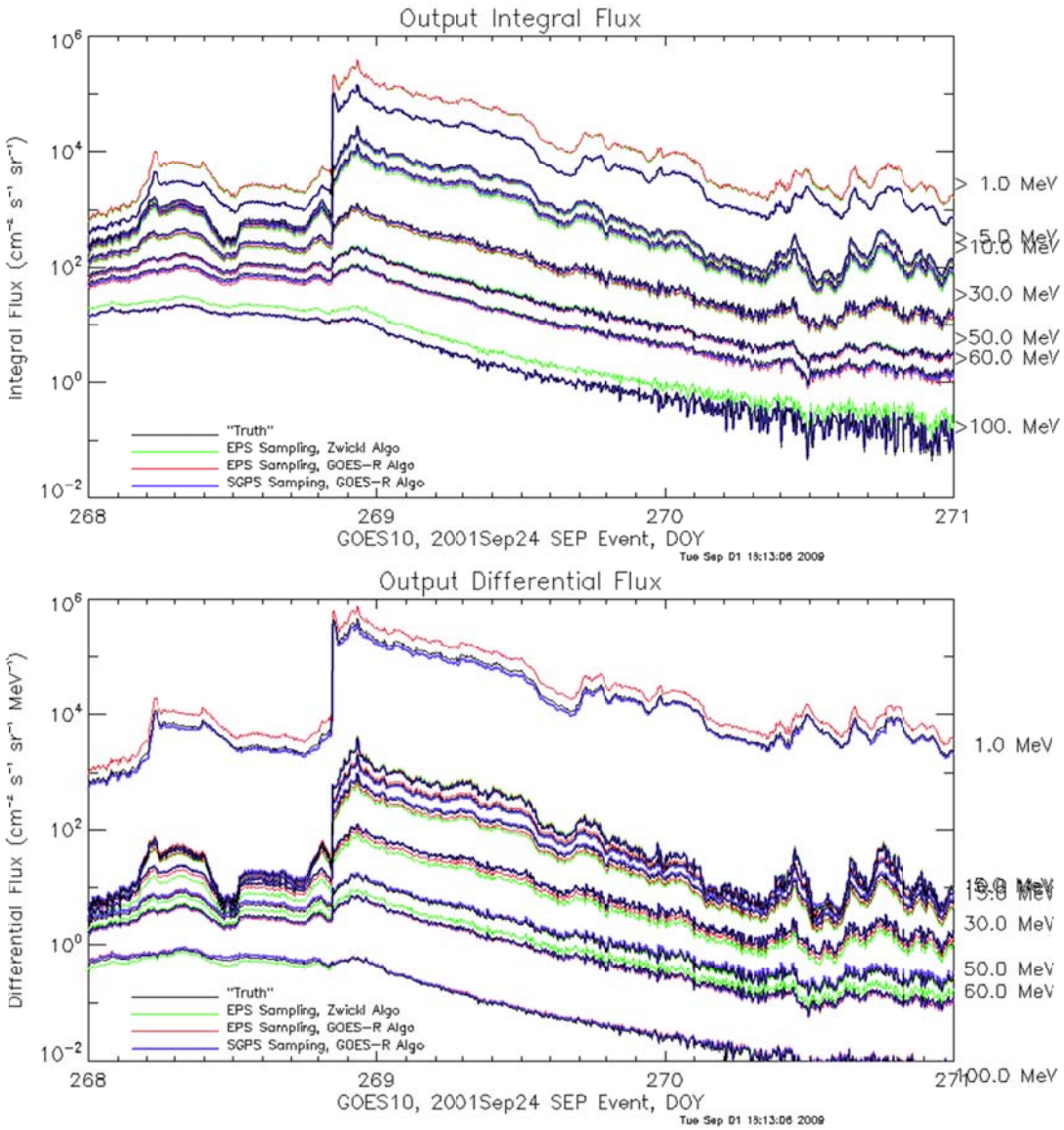

Figure 7. Comparison of integral flux and differential flux retrievals to "truth" for the GOES 10 eastward observations of solar protons during the September 24, 2001 SEP event. The "truth" is derived from fits to the GOES 10 data using a combined kappa distribution and power law distribution. The format of the figure is similar to that of Figure 6.

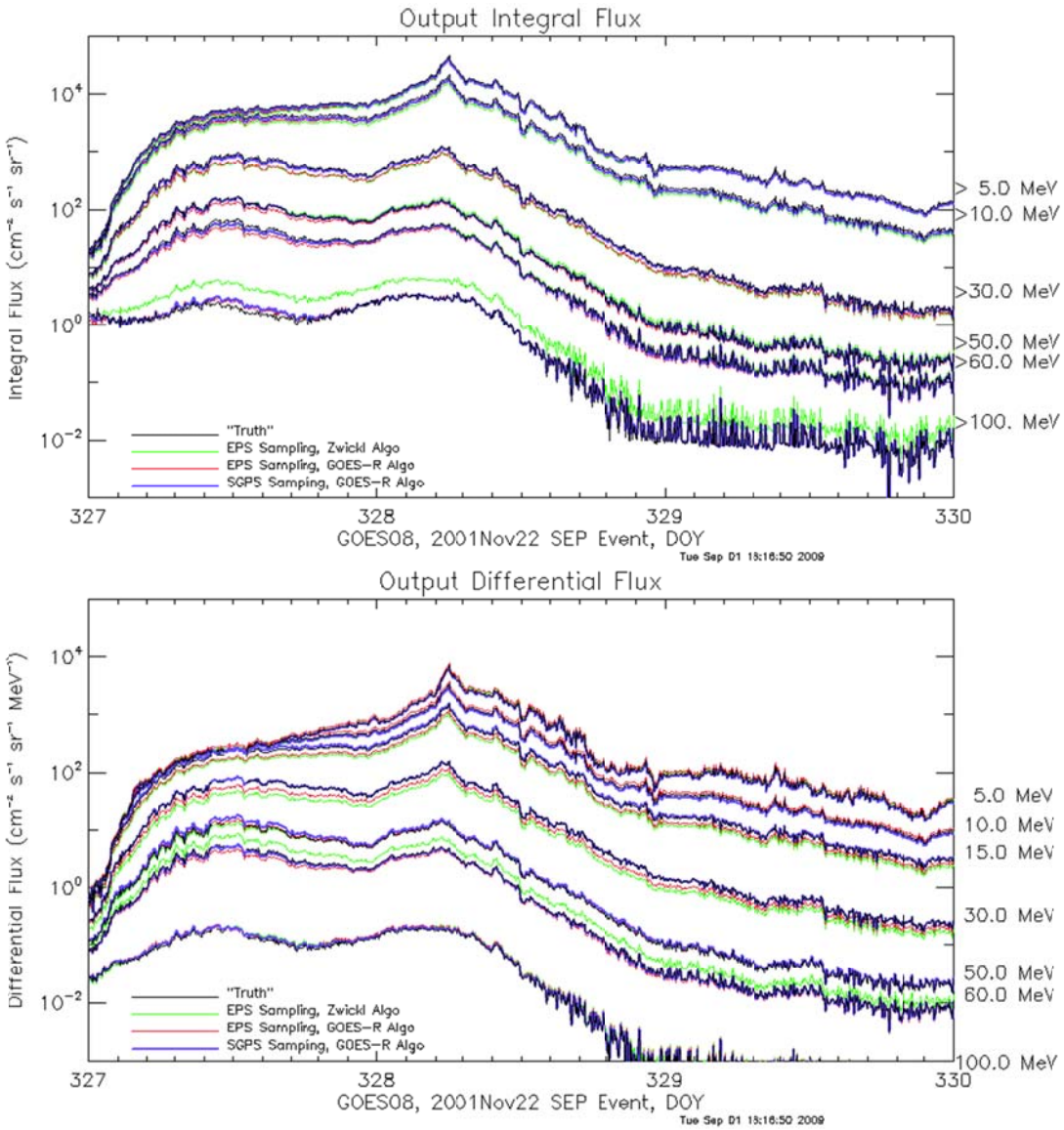

Figure 8. Comparison of integral flux and differential flux retrievals to "truth" for the GOES 8 westward observations of solar protons during the November 22, 2001 SEP event. The "truth" is derived from fitting a kappa distribution to the GOES 8 data. The format of the figure is similar to that of Figure 6.

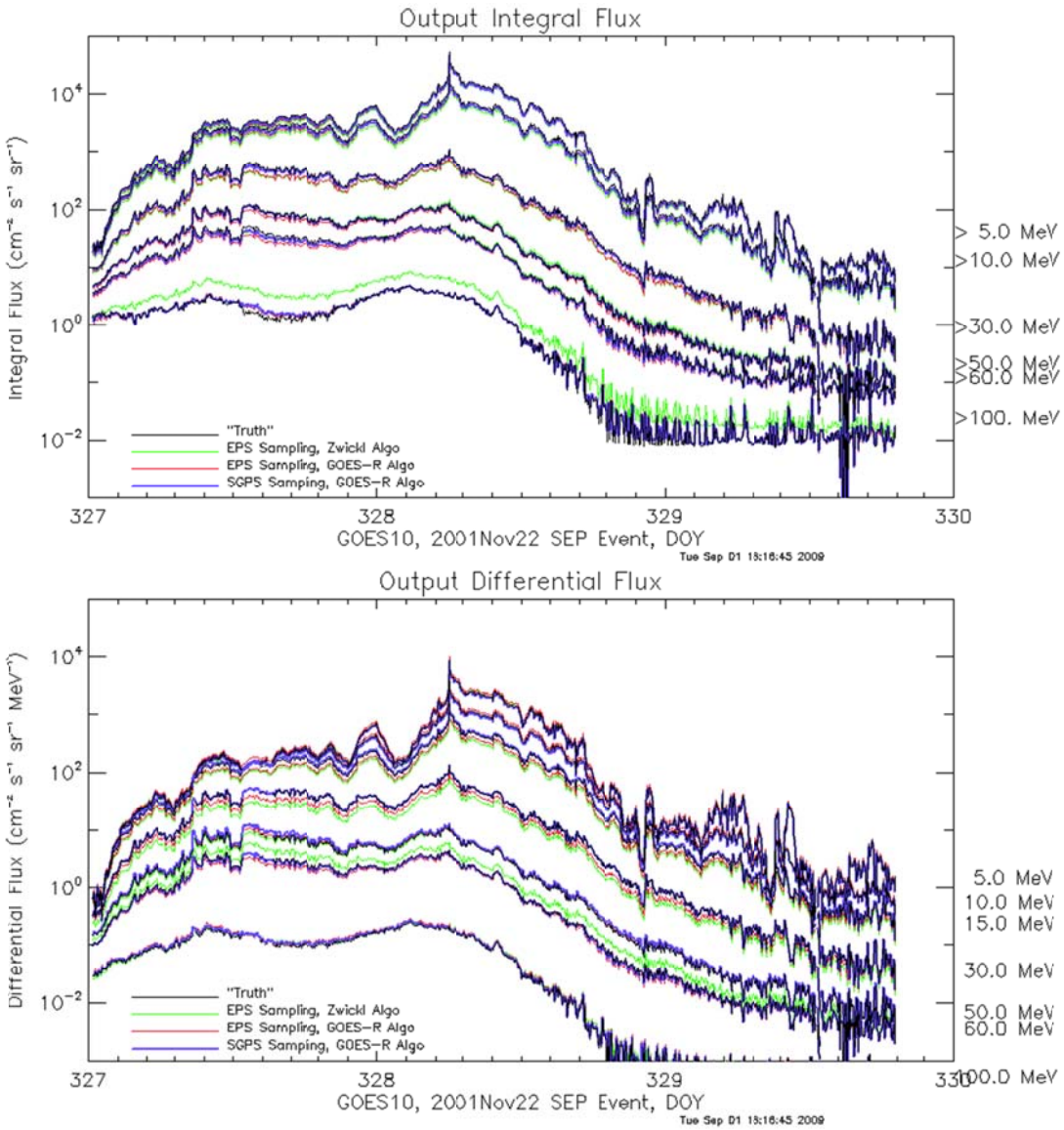

Figure 9. Comparison of integral flux and differential flux retrievals to "truth" for the GOES 10 eastward observations of solar protons during the November 22, 2001 SEP event. The "truth" is derived from fitting a kappa distribution to the GOES 10 data. The format of the figure is similar to that of Figure 6. Data gaps indicate where the fits were not calculated because the differential flux in the P2 channel was less than 1 proton / (cm2 s sr MeV).

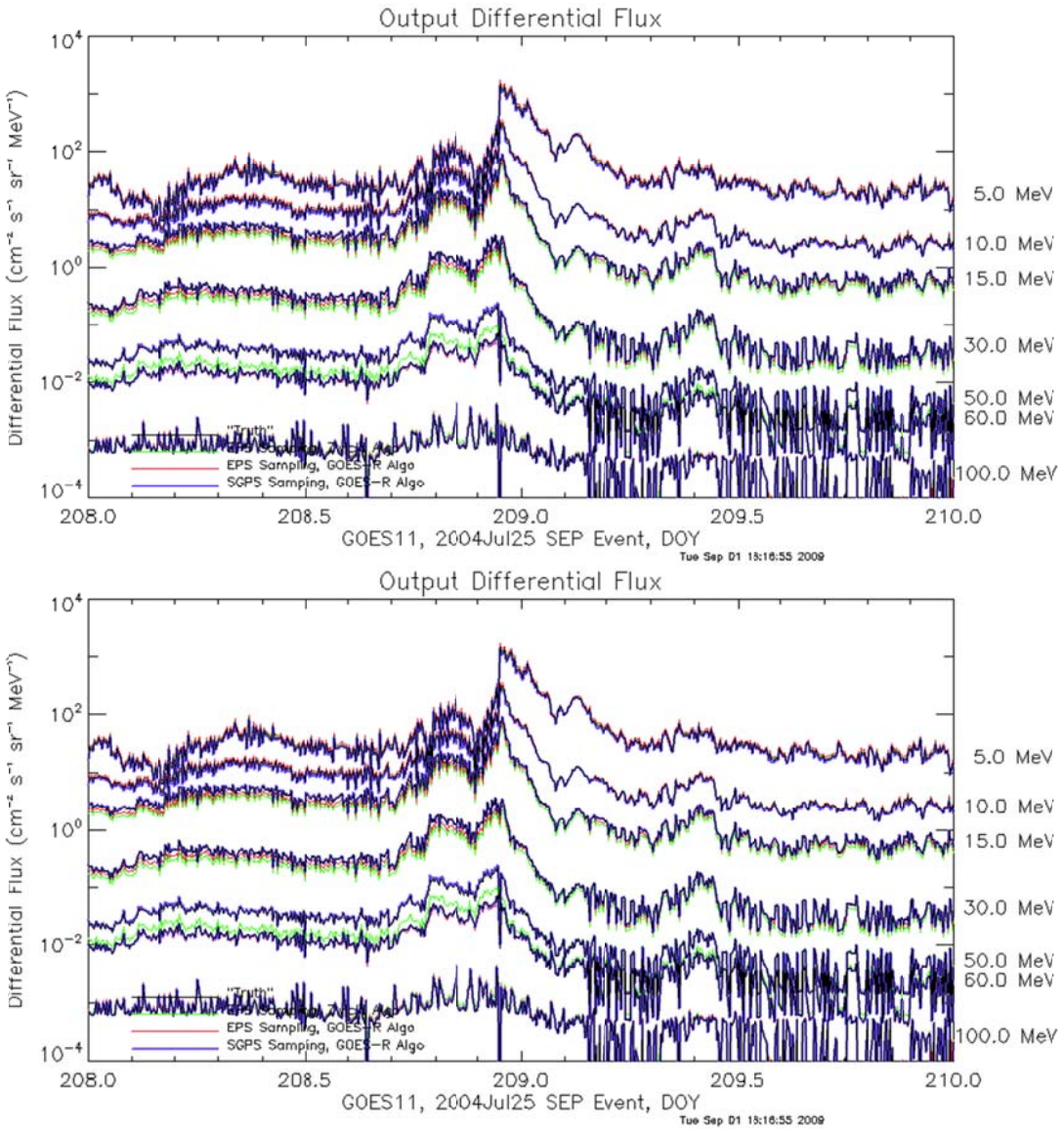

Figure 10. Comparison of integral flux and differential flux retrievals to "truth" for the GOES 11 westward observations of solar protons during the July 25, 2004 SEP event. The "truth" is derived from fitting a kappa distribution to the GOES 11 data. The format of the figure is similar to that of Figure 6.

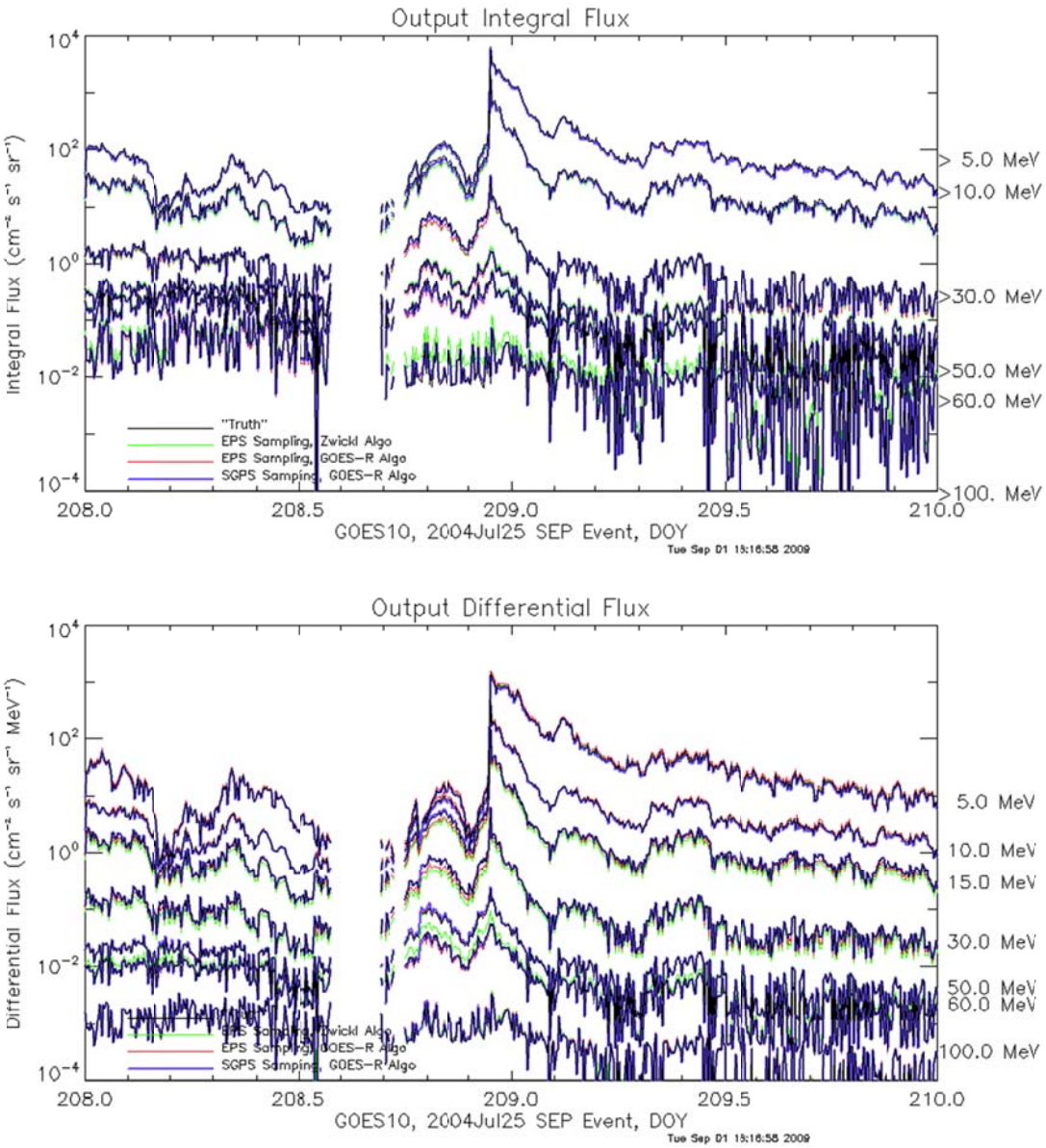

Figure 11. Comparison of integral flux and differential flux retrievals to "truth" for the GOES 10 eastward observations of solar protons during the July 25, 2004 SEP event. The "truth" is derived from fitting a kappa distribution to the GOES 10 data. The format of the figure is similar to that of Figure 6. Data gaps indicate where the fits were not calculated because the differential flux in the P2 channel was less than 1 proton / (cm2 s sr MeV).

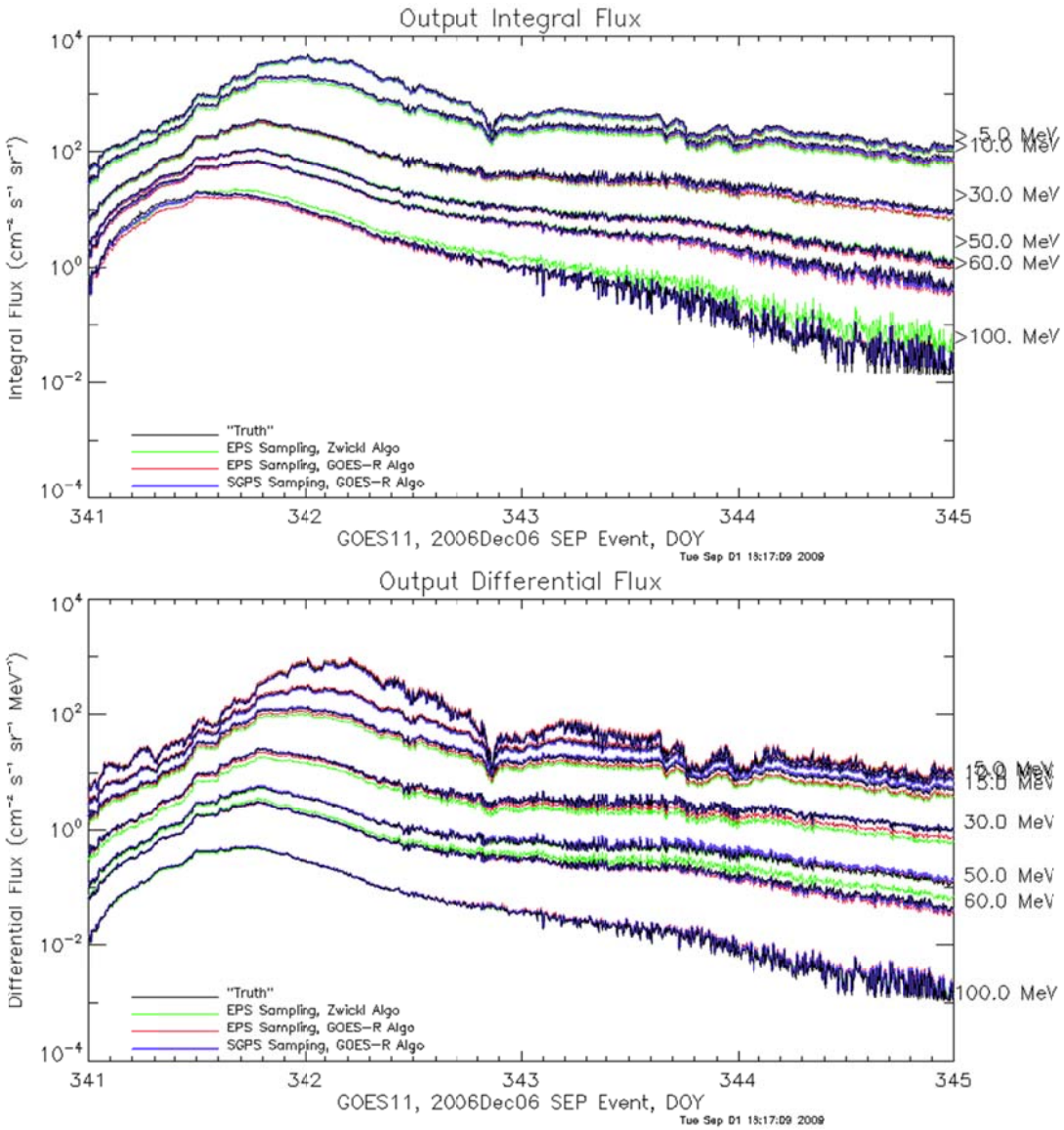

Figure 12. Comparison of integral flux and differential flux retrievals to "truth" for the GOES 11 westward observations of solar protons during the December 6, 2006 SEP event. The "truth" is derived from fitting a kappa distribution to the GOES 11 data. The format of the figure is similar to that of Figure 6.

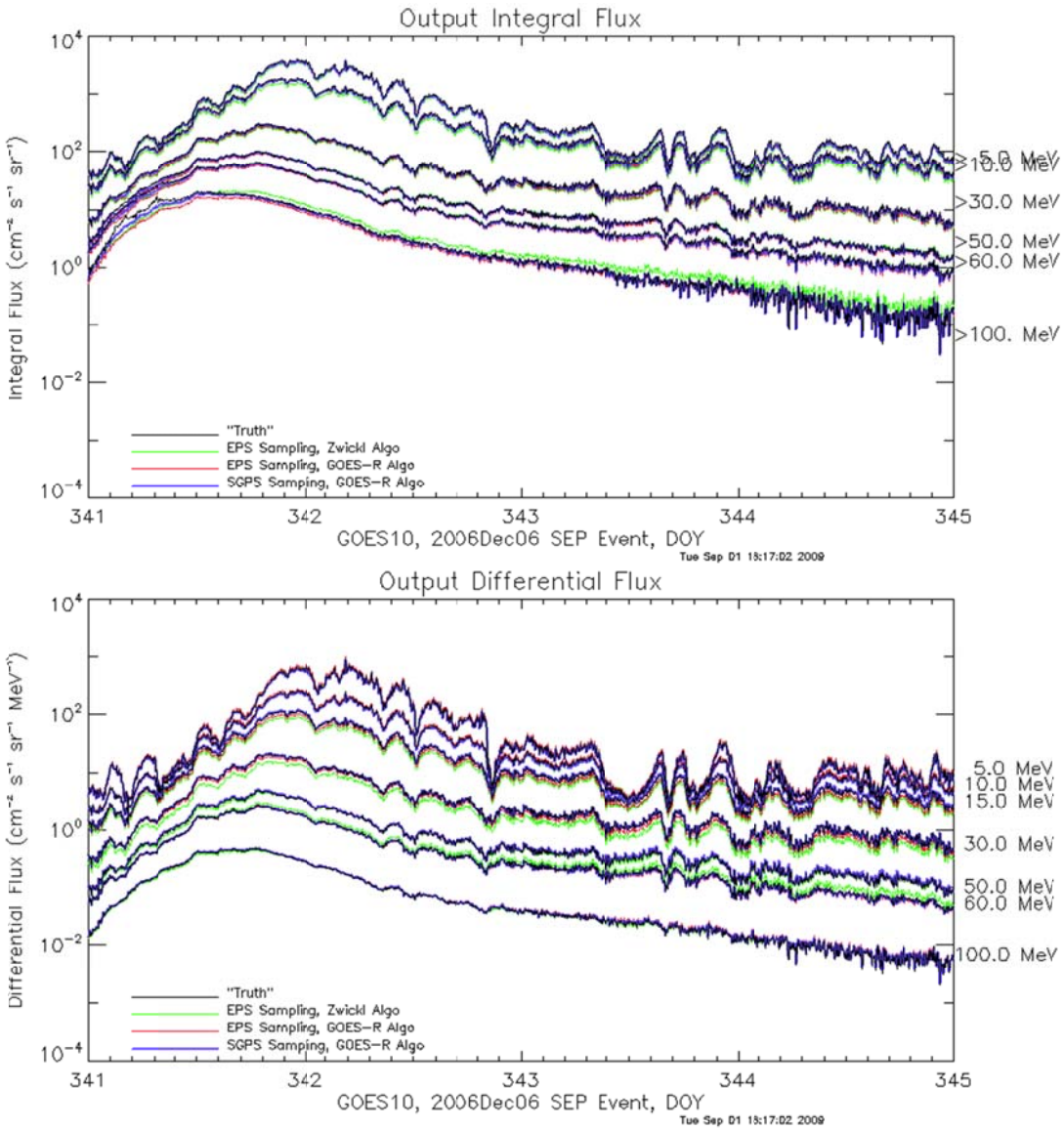

Figure 13. Comparison of integral flux and differential flux retrievals to "truth" for the GOES 10 eastward observations of solar protons during the December 6, 2006 SEP event. The "truth" is derived from fitting a kappa distribution to the GOES 10 data. The format of the figure is similar to that of Figure 6.

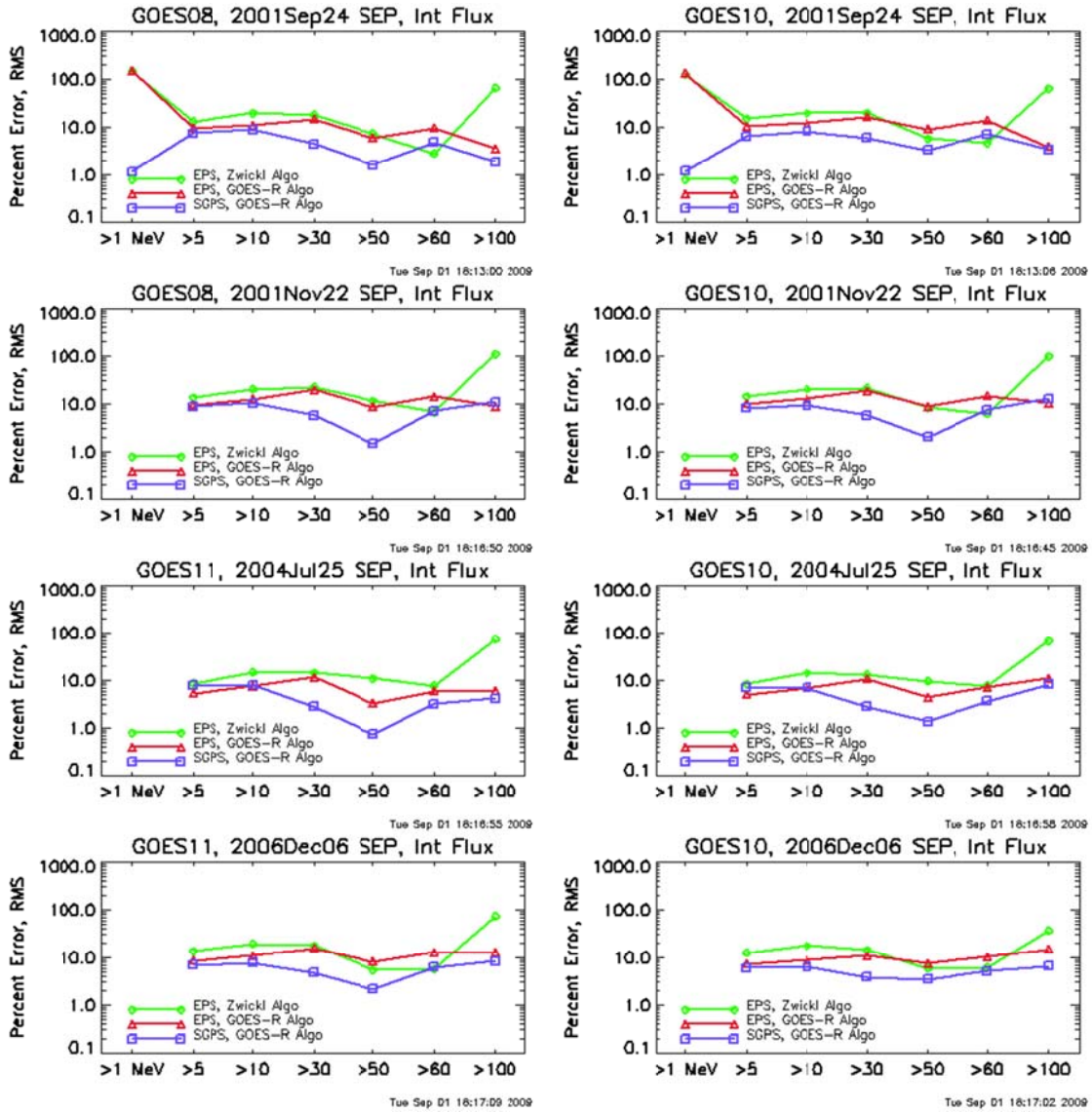

Figure 14. Percent RMS error for each of the integral flux retrievals shown in Figure 6 through Figure 13. The RMS error is determined over the entire event plotted in each figure relative to the "truth." The green curves represent the retrievals by the Zwickl [1989] algorithm. The red curves represent the GOES R algorithm retrievals using data at the GOES I-P EPS/EPEAD spectral resolution. The blue curves represent the GOES R algorithm retrievals using data at the SGPS spectral resolution. The error for each retrieval is normalized by the true integral flux prior to being combined with the other errors in the RMS estimate. The error in the >1 MeV fluxes was determined only for the September 24, 2001 cases.

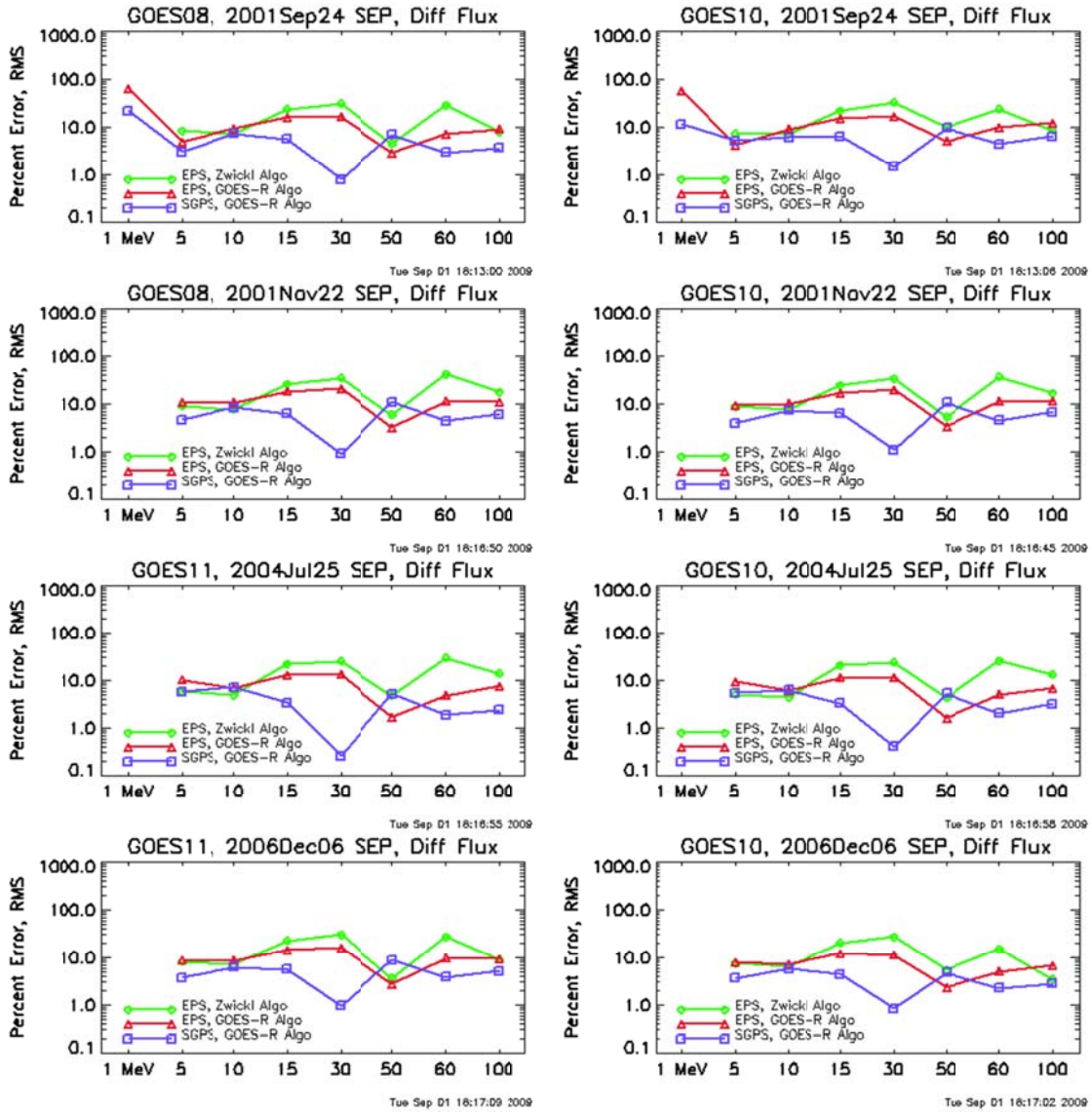

Figure 15. Percent RMS error for each of the differential flux retrievals shown in Figure 6 through Figure 13. The RMS error is determined over the entire event plotted in each figure relative to the "truth." The green curves represent the retrievals by the Zwickl [1989] algorithm. The red curves represent the GOES R algorithm retrievals using data at the GOES I-P EPS/EPEAD spectral resolution. The blue curves represent the GOES R algorithm retrievals using data at the SGPS spectral resolution. The error for each retrieval is normalized by the true differential flux prior to being combined with the other errors in the RMS estimate. The error in the 1 MeV fluxes was determined only for the September 24, 2001 cases, and not for the Zwickl [1989] algorithm, which does not calculate the 1 MeV differential fluxes.

The basic conclusion drawn from this analysis is that both the GOES I-P and GOES R algorithm are susceptible to undersampling errors in spectral regions where gamma is varying rapidly. The improved spectral sampling of the GOES R SGPS relative to GOES I-M EPS and GOES N-P EPEAD should improve the accuracy of the integral fluxes with respect to the "true" spectrum. All else being equal, however, the GOES R "iterative" algorithm improves performance over the GOES I-P algorithm. This is probably due to the fact that there is inherent geophysical variability about the forward model curve fits used in the older algorithm that is partially corrected for by the iterative solution in the newer algorithm.

The magnitude of the improvement can only be approximated by analyses such as these that use imperfect representations of the actual spectrum. Since the curve fits used here are smoothed versions of the true spectra, the errors presented here are probably underestimates. However, within their obvious limitations, these simulations demonstrate the improvements to be expected in the GOES R Differential-to-Integral Flux products due to the improved spectral sampling of the SGPS and the algorithm designed to work with it.

5.0 PRACTICAL CONSIDERATIONS

5.1 Numerical Computation Considerations

The algorithm is straightforward to implement in software. The retrievals do not require matrix inversions. The most complex part of the algorithm, the iterative solution for the channel center energies and gammas, is limited in the number of iterations that can take place. Though the measurements are single precision, the calculations should take advantage of the double precision capabilities of the host machine.

5.2 Programming and Procedural Considerations

The operational algorithm has been implemented in C++. It uses four classes related to the background counts, the channel energies, the exponential factor gamma (γ), and the particle fluxes. These classes include many member functions in order to maintain the readability and modularity of the code.

5.3 Quality Assessment and Diagnostics

Quality assessment of the operational product is based on the flags described in the next section. If hasMissingFlux is set frequently, then either the instrument is

having problems or there is a problem upstream in the data processing system. The default gammas will be set frequently outside of SEP events. The gamma limits should be invoked less frequently. Based on testing with the proxy data, the energy iteration limit should be reached very infrequently.

The classes include member functions for printing out intermediate values in order to facilitate diagnostics.

5.4 Exception Handling

It is assumed that the majority of the error handling is performed by the averaging algorithms which provide the input to this calculation. Any measurement gaps or bad data should be flagged in the input and disregarded by this algorithm. This algorithm requires a complete set of 5-minute averaged differential flux values to accurately represent the flux - energy spectrum. Checks on the validity of the input, based on bad data flags from the 5-minute average proton differential flux routine, and threshold levels for the input will be made by this algorithm.

In the presence of one or more missing differential flux values (assumed to be indicated by fill value -99999.), the algorithm will not calculate the integral flux. Instead, it sets the output integral flux to -99999. and hasMissingFlux to 1. In principle, it is possible to interpolate or extrapolate over a missing flux value. However, there are many possible permutations of missing flux values, and each could require a different algorithm. If the problem is random and infrequent, then it is not worthwhile to develop an algorithm to handle the problem. Should one or more channels in a given westward-looking SGPS fail, and its eastward-looking partner have similar problems, and the solar proton measurements not be available from another GOES satellite, then it may be possible to develop an algorithm to handle the specific situation.

The flag isBackground is a 9-element vector corresponding to the energy intervals between the centers of the differential channels. If gamma is set to the default values (Table 6) for a given interval, the corresponding element of isBackground is set to 1; otherwise, the elements of isBackground are 0. This flag is useful for identifying whether measurements are at or near the background levels.

The flag hasGammaLimit is a 9-element vector corresponding to the energy intervals between the centers of the differential channels. If gamma is set to one of the two acceptable range limits (-8 or +8) for a given interval, the corresponding element of hasGammaLimit is set to 1; otherwise, the elements of hasGammaLimit are 0. If this flag is set, it could indicate an unusual event, or perhaps a problem in the measurements.

The flag isNotConverged is a 10-element vector corresponding to the ten differential energy channels, initialized to 1. If, for the center energy E_i of an individual energy channel, the number of iterations required to reach the convergence criterion is less than the permitted number of iterations, then this flag is set to 0. If, for a given channel, the center energy has not converged after the permitted number of iterations, the process is stopped and the flag remains 1.

5.5 Algorithm Validation

The L1b solar proton measurements can be intercalibrated with measurements at other local times. (Note that eastward measurements can only be intercalibrated with eastward measurements, and likewise for westward observations.) Once the L1b fluxes have been validated, the L2 outputs of this algorithm can be validated by comparison with simultaneous measurements by the EPEAD instruments on the prior GOES-NOP series. Based on the simulations shown earlier, one can expect factor of 2 differences in the >1 MeV and >100 MeV integral fluxes, due to the improved spectral sampling by the SGPS and improvements in the algorithm. However, in general agreement should be better than this. A validation exercise should include running the GOES-NOP fluxes through the GOES R algorithm.

In the absence of SEP events, the >1 MeV integral flux and 1 MeV differential flux outputs can still be evaluated. One should expect greater scatter in these comparisons than with SEP event fluxes due to the limited spectral sampling (only one contributing channel, P1) in the earlier instruments.

Care should be taken to account for differences in the angular response of the EPEAD and SGPS instruments, should they be significant.

6.0 ASSUMPTIONS AND LIMITATIONS

6.1 Instrument Characteristics

The instrument characteristics used by the algorithm include the channel upper and lower energies and geometrical factors (Table 3). They are labeled as ancillary data in this document, but this could change as the definition of calibration data within the GOES R system matures. The quantity "geometrical factors" is in fact the product of several tabulated quantities, including:

1. the geometrical factors derived from ground calibration data;
2. relative responses derived from intercalibrations of the responses of different telescopes during on-orbit cal/val (including yaw flips);
3. adjustments from satellite intercomparisons during on-orbit cal/val; and
4. adjustments from the results of in-flight calibrations over the life of the mission.

All but the first table will be "unity" at the time of launch.

It is assumed that STAR, being responsible for L1b cal/val, will maintain and update these separate tables and create the product of these tables.

The L1b and L2 algorithms must use the same channel energies and geometrical factor tables.

6.2 Instrument Constants to be Re-evaluated after Cal/Val

The following constants must be re-evaluated following SEISS SGPS ground calibration and characterization and after on-orbit calibration and validation of the L1b and L2 products.

From L1b cal/val:

Channel upper and lower energies (Table 6) and geometrical factors (actually GΔE, Table 6)

From L2 cal/val:

Default gammas, upper limits to background count rate, and background count rate seed for running average (Table 6)

6.3 Input and Output File Contents and Formats

As of September 2009, the contents of the SGPS L1b files have not been defined by the SEISS contractor. The assumed data (averaged by the averaging algorithm) and metadata (passed through by the averaging algorithm) are given in Table 1 and Table 2. For more information, see the discussion associated with these tables.

The input averaged L1b channel differential fluxes are assumed to be the first-order estimates calculated as

$$j_i = \frac{C_i}{G_i\left(E_{u,i} - E_{l,i}\right)}$$

where C_i is the corrected count rate in channel i, G_i is the geometrical factor (cm^2 sr), and E_l and E_u are the lower and upper energies of the channel (MeV). This is the practice for prior GOES satellites. If this assumption is not correct, then the iterative solution for the channel energies may not be valid.

The running average used to estimate the background contamination levels assumes that the input averaged L1b files are time-ordered.

The outputs of the Differential-to-Integral Flux L2 algorithm are listed in Table 7. As of September 2009, it is not known whether the westward- and eastward-observed fluxes and flags will be output in one record or in separate records. Currently, the algorithm assumes that the East and West L1b records are separate, and therefore the East and West L2 outputs are separate.

6.4 Performance

The product measurement accuracy of the solar and galactic protons differential fluxes is set in the MRD (3.3.6.1.4) to have a threshold of 25%, including the contributions of Monte Carlo analysis to the calibrations. This requirement has been flowed down to the SEISS PORD for SGPS. This 25% accuracy requirement refers to the ground calibration accuracy requirement for SGPS, and cannot be verified on-orbit. If the instrument is calibrated correctly and meets its accuracy requirements, this fulfills this L2 product's accuracy requirement. There is no equivalent precision requirement.

In addition, the SEISS PORD specifies that the response to out-of-band particles (including direction, energy range, and species) is to be no more than 10% of the response to in-band particles, after ground processing. This is a very important requirement as out-of-band contamination is a major factor in the performance of these types of measurements. The performance of the out-of-band correction will have a direct influence on the quality of the Differential-to-Integral Flux product.

An important performance parameter is continuity of integral flux levels between satellites. Satellite-satellite intercomparisons are needed to ensure continuity of the operational product. Such intercomparisons have been successful on GOES 8-12, and they need to be worked into the GOES-R program, possibly as part of cal/val. These intercomparisons need to be made at the L1b corrected flux level.

Generally, there has been good continuity in the performance of the GOES I-P EPS/EPEAD solar proton measurements, but SGPS is a new design and we can expect discontinuities in performance, at least initially. If the L1b fluxes agree, one can still expect systematic differences in the L2 products as described above under “Algorithm Validation,” due to improvements in the sensor and the algorithm. It would be incorrect, however, to regress the new measurements to the old levels in the presence of large systematic differences without any physical basis for doing so.

6.5 Pre-Planned Product Improvements

Currently, the only metadata from the averaged L1b records that are passed through to the L2 records are the time stamp and the FOV center direction cosines (Table 1), and they are not used to calculate the integral fluxes. When the SEISS L1b metadata are defined, consideration should be given to passing other useful information such as spacecraft location and orientation (Table 2) through to the L2 records, in order to make the L2 data more “stand-alone”.

Alternative spectral retrieval methods may be considered if they are validated on upcoming science missions such as Radiation Belt Storm Probes (RBSP). RBSP-GOES intercomparisons may play a valuable role in algorithm validation.

7.0 REFERENCES

Armstrong, T. P., CPME Data Handbook for IMP 7, I. Proton-Electron-Telescope Parameters, Johns Hopkins University Applied Physics Laboratory, 1972.

Armstrong, T. P., Handbook and Reference Manual for Charged Particle Measurement Experiment Data from Explorer 47 and 50, Johns Hopkins University Applied Physics Laboratory, 1976.

Baker, D. N., Solar wind-magnetosphere drivers of space weather, *J. Atmos. Terr. Phys., 58*, 1509-1526, 1996.

Baker, D. N., R. D. Belian, P. R. Higbie, and E. W. Hones, Jr., High-energy magnetospheric protons and their dependence on geomagnetic and interplanetary conditions, *J. Geophys. Res., 84*, 7138-7154, 1979.

Bryant, D. A., T. L. Cline, U. D. Desai, and F. B. McDonald, Explorer 12 observations of solar cosmic rays and energetic storm particles after the solar flare of September 28, 1961, *J. Geophys. Res., 67*, 4983-5000, 1962.

Cane, H. V., and D. Lario, An introduction to CMEs and energetic particles, *Space Sci. Rev., 123*, 45-56, 2006.

Christon, S. P., D. G. Mitchell, D. J. Williams, L. A. Frank, C. Y. Huang, and T. E. Eastman, Energy spectra of plasma sheet ions and electrons from ~50 eV/e to ~1 MeV during plasma temperature transitions, *J. Geophys. Res., 93*, 2562-2572, 1988.

Fritz, T. A., and 22 coauthors, Significant initial results from the Environmental Measurements Experiment on ATS-6, *NASA Technical Paper 1101*, December 1977.

Lario, D., and R. B. Decker, The energetic storm particle event of October 20, 1989, *Geophys. Res. Lett., 29*, 10.1029/2001GL014017, 1002.

O'Brien, T. P., SEAES-GEO: A spacecraft environmental anomalies expert system for geosynchronous orbit, *Space Weather, 7*, 10.1029/2009SW000473, 2009.

Press, W. H., B. P. Flannery, S. A. Teukolsky, and W. T. Vetterling, *Numerical Recipes in C: The Art of Scientific Computing*, Cambridge University Press, 1988.

Sauer, H. H., and D. C. Wilkinson, Global mapping of ionospheric HF/VHF radio wave absorption due to solar energetic protons, *Space Weather, 6*, 10.1029/2008SW000399, 2008.

Vasyliunas, V. M., A survey of low-energy electrons in the evening sector of the magnetosphere with OGO 1 and OGO 3, *J. Geophys. Res., 73,* 2839-2884, 1968.

Zwickl, R., GOES-7 Energetic Particle Algorithm, unpublished technical note, 1989.